

Clustering in Small Networks of Excitatory Neurons with Heterogeneous Coupling Strengths

Yue-Xian Li^(1,2), Yuqing Wang^(1,3), and Robert M. Miura^(1,4)

⁽¹⁾ Department of Mathematics and
Institute of Mathematical Sciences

University of British Columbia, Vancouver, BC Canada V6T 1Z2

⁽²⁾ Department of Zoology, University of British Columbia
Vancouver, BC Canada V6T 1Z2

⁽³⁾ Pacific Institute for the Mathematical Sciences
University of British Columbia, Vancouver, BC Canada V6T 1Z2

⁽⁴⁾ Departments of Mathematical Sciences and
Biomedical Engineering and
Center for Applied Mathematics and Statistics
New Jersey Institute of Technology, Newark, NJ 07102 USA

CAMS Report 0203-25, Spring 2003

Center for Applied Mathematics and Statistics

NJIT

Clustering in Small Networks of Excitatory Neurons with Heterogeneous Coupling Strengths

Yue-Xian Li^{1,2}, Yu-qing Wang¹, and Robert Miura^{1,3,4}

Departments of ¹Mathematics, ²Zoology, ³Pharmacology & Therapeutics,
University of British Columbia, Vancouver, BC, Canada V6T 1Z2

⁴Departments of Mathematical Sciences and Biomedical Engineering
New Jersey Institute of Technology, Newark, NJ 07102, USA

July 26, 2002

Correspondence:

Prof. Yue-Xian Li

Tel: 604-822-6225

Department of Mathematics, University of British Columbia

Fax: 604-822-6074

#121-1984 Mathematics Road, Vancouver, BC, Canada, V6T 1Z2

Email: yxli@math.ubc.ca

Acknowledgements

This work was financially supported by NSERC (Natural Sciences and Engineering Research Council of Canada) grants to Y.X.L. and R.M.M., and partially by a PIMS (Pacific Institute for the Mathematical Sciences) fellowship to Y.Q.W.

Abstract

Excitatory coupling with a slow rise time destabilizes synchrony between coupled neurons. Thus, the fully synchronous state is usually unstable in networks of excitatory neurons. Phase-clustered states, in which neurons are divided into multiple synchronized clusters, have also been found unstable in numerical studies of excitatory networks in the presence of noise. The question arises as to whether synchrony is possible in networks of neurons coupled through slow, excitatory synapses. In this paper, we show that robust, synchronous clustered states can occur in such networks. The effects of non-uniform distributions of coupling strengths are explored. Conditions for the existence and stability of clustered states are derived analytically. The analysis shows that a multi-cluster state can be stable in excitatory networks if the overall interactions between neurons in different clusters are stabilizing and strong enough to counter-act the destabilizing interactions between neurons within each cluster. When heterogeneity in the coupling strengths strengthens the stabilizing inter-cluster interactions and/or weakens the destabilizing in-cluster interactions, robust clustered states can occur in excitatory networks of all known model neurons. Numerical simulations were carried out to support the analytical results.

Running title: Clustering in networks with non-uniform coupling strengths

Keywords: Neural networks, Synchronization, Phase locking, Phase clustering, Coupled oscillators

1 Introduction

Neurons in a functioning brain are constantly interacting with each other. For this reason, coherence and correlation in the electrical activities between neurons are of great importance in understanding the function of a large network of neurons. Rhythms in the electroencephalogram (EEG) are the best known examples of synchronous electrical activities of a large number of interacting neurons. Several such rhythms have been associated with different physiological and pathological states of the brain (Traub *et al.*, 1999). Hormone secreting neurons in the hypothalamus are found to release hormones in a pulsatile manner, and such pulsatility often is related to synchrony in the electrical activities of these neurons (Leng, 1988; Knobil, 1987). Animal locomotion is also known to be controlled, in part, by networks of neurons capable of generating coordinated output (Grillner, 1975). It is believed that information in the brain is coded in the firing rate of individual neurons as well as in the spatiotemporal firing pattern of a network of neurons in which spike-to-spike correlation is of key importance (Abbott, 1994; Gray *et al.*, 1989). A rich variety of activity patterns have been observed including synchronized oscillations and propagating waves (Gutnik *et al.*, 1982; Smith *et al.*, 1991; Gray, 1994; Nicolelis *et al.*, 1995; Prechtl *et al.*, 1997; Reckling and Feldman, 1998). Because of the highly nonlinear nature of these activity patterns, mathematical modeling has become an important tool in studying these patterns.

Synchrony and phase-locking between coupled neurons have been studied extensively. Early studies showed excitatory coupling leads to synchrony while inhibitory coupling leads to asynchrony (Winfrey, 1967; Kuramoto, 1984; Ermentrout and Kopell, 1984; Glass and Mackey, 1988; Mirollo and Strogatz, 1990). This result was later contradicted by many case studies both experimental and numerical (Sortie and Rand, 1986; Lytton and Sejnowski, 1991; Sherman and Rinzel, 1992;

Wang and Rinzel, 1992; Steriade *et al.*, 1993; Golomb *et al.*, 1994). Theoretical explanation of this contradiction has been provided based on the theory of weakly coupled oscillators (Van Vreeswijk *et al.*, 1994; Hansel *et al.*, 1995). It was shown that the time scales of the rise and decay of synaptic currents are of crucial importance. When the coupling is not fast, excitatory coupling leads to asynchrony while inhibitory coupling promotes synchrony. Synaptic coupling between neurons is not instantaneous. Therefore, synchrony in networks of globally coupled neurons is often destroyed by excitatory synapses. This is true for both the fully synchronous state and partially synchronous, phase-clustered states in which neurons are self-organized into synchronous clusters with fixed inter-cluster phase differences (Golomb *et al.*, 1992; Golomb and Rinzel, 1994; Van Vreeswijk, 1996; Ernst *et al.*, 1998). Stable phase-clustered states have mostly been found numerically in networks of inhibitory neurons (Golomb and Rinzel, 1994; Hansel *et al.*, 1995; Van Vreeswijk, 1996; Ernst *et al.*, 1998). In excitatory networks, such states have been reported occasionally (Hansel *et al.*, 1995; Ernst *et al.*, 1998); however, they were not robust in the presence of small noise.

These results raised the question as whether synchrony is possible in networks of neurons coupled through slow excitatory synapses. We here present a theory on whether and how synchrony is possible even interactions between synchronized neurons are destabilizing. Heterogeneity in the coupling strengths is considered in the study since it plays an important role in stabilizing phase-clustered states. To make the analysis tractable, we focus on small networks of four and six neurons. The analysis is based on the reduced phase description of coupled oscillators. When the coupling is “weak”, which happens to be true in many realistic systems, each oscillator can be approximated by one single phase equation in which interaction between two oscillators is described by a nonlinear

function of the phase difference between the two. Thus, a network of N neurons is described by a system of N phase-coupled differential equations. We then derive the $N - 1$ differential equations of independent phase differences. Phase-locked states are steady state solutions to these equations. Phase-clustered states are special phase-locked states in which neurons within each cluster are locked at zero phase difference. This approach has been used previously (Ermentrout and Kopell, 1984; Williams *et al.*, 1990). One difficulty in studying the dynamics of a network of multiple neurons is the co-existence of many possible solutions. In general, we cannot predict the exact number of solutions since this number depends on specific properties of the individual neurons in the network. However, many interesting solutions of a network (including the clustered states in the present study) occur due to symmetries in the network, thus are independent of specific properties a single neuron. Such states are referred to as model-independent states. Thus, we select some special distributions of coupling strengths with certain symmetries that favor the occurrence of phase-clustered states. We then construct solutions that possess these symmetries. These solutions are substituted into the equations to determine conditions for their existence and stability.

In Section 2, we introduce the concept of *selective heterogeneity* in the distribution of coupling strengths. In Sections 3 and 4, we derive the conditions for the existence and stability of phase-clustered solutions for some special distributions of coupling strengths. In Section 5, we apply the theory to small networks of two current-based models as well as the integrate-and-fire (IF) model. Numerical simulations are carried out to confirm the analytical predictions. In Section 6, we study the co-existence of model-independent phase-locked states in the four-neuron network and show how the fine tuning of coupling strengths selectively favors different states in the presence of noise.

In Section 7, we summarize the results and discuss possible extensions and potential applications.

2 Selective heterogeneity in the coupling strength

In this paper, we study globally coupled neurons with heterogeneous coupling strengths. Each neuron can be coupled to different neurons with different strengths. Heterogeneous coupling has been studied previously in several cases. Thus, nearest neighbor coupling is heterogeneous since the coupling strength is nonzero only between neighboring neurons. Distance-dependent distribution also is heterogeneous since the coupling strength is different for neurons at different distances. In our study, heterogeneity is neither stochastic nor irregular but is highly selective. This is based on the assumption that a distinctive coupling strength between two neurons often is determined by their functional relationship. Selective heterogeneity can occur as a result of activity-dependent potentiation associated with the repetition of certain sensory signals. Selective coupling, as we shall demonstrate later, allows the network to evolve selectively into one of the co-existing phase-clustered states. We believe selective heterogeneity is likely to occur in a realistic network because synaptic coupling between real neurons is constantly being modified due to short-term and long-term neural plasticity. As we shall illustrate later, selective variability in the coupling strength can stabilize (or destabilize) certain phase-clustered states that are otherwise unstable (stable). We introduce this concept to facilitate the development of a theory in which the coupling strength plays a key role in the stability of phase-locked states. The idea is to incorporate coupling strengths into the conditions that determine the stability of phase-locked states. This makes it possible for a network to change from one state to another by appropriately adjusting the coupling strengths.

Take the example of a network of four neurons. The total number of connections is $\binom{4}{2} = 6$.

For simplicity, we assume that coupling between any pair of neurons is identical in both directions. It is either excitatory or inhibitory but not a mixture of the two. We only consider heterogeneous distributions of coupling strengths that retain enough symmetry to allow model-independent phase-clustered states to occur. Fig. 1 shows two heterogeneous distributions of coupling strength in a four-neuron network, the triangle and the square distributions. Here, physical distance is used as a measure of the coupling strength. In real neural networks, coupling strength is not necessarily determined by physical distance. The concept of *distance* can be generalized to include *functional distance*, e.g. the degree of correlation in the activity of coupled neurons. In the triangle distribution (Fig. 1a), three neurons are located at the vertices of a triangle and one in the center. Distances between neurons at the vertices are different from their distances to the neuron at the center. In the square distribution (Fig. 1b), four neurons are located at the corners of a square. Each neuron is coupled to its nearest neighbors with one coupling strength, w_O , but to its diagonal neighbor with a different strength, w_I .

For a network in which neurons are located at certain distances from each other, the distribution of coupling strength is determined by the functional relationship between the distance, R , and the coupling strength, W . Fig. 2 gives several possible examples of $W(R)$. Coupling strength can decrease exponentially as distance increases (Fig. 2a). Discrete distribution of coupling strength may occur if thresholds exist such that the coupling strength changes little for distances between these thresholds (see Figs. 2b,c). Fig. 2b shows a centered distribution with a cut-off threshold distance R_c . Fig. 2c gives an annular (off-centered) distribution with two thresholds, R_{c1} and R_{c2} . The coupling strength is larger at distances between the two thresholds.

3 Phase-clustered states in a network of four neurons

In this study, the definition of a phase-clustered state is restricted to the states in which neurons are divided into $n \geq 2$ clusters with each cluster containing $n_s \geq 2$ neurons. This excludes the “splay-phase” state (Nichols and Wiesenfeld, 1992) in which the phases of all neurons are distinct and evenly distributed and the one-cluster state that is simply the fully synchronized state. Thus, the smallest possible network in which such a phase-clustered state can occur is a four-neuron network.

The reduced phase description of a weakly-coupled four-neuron network is given by (12) in Appendix A for $N = 4$. Phase-locked states are steady-state solutions of differential equations for the phase differences. For a network of four neurons, there are a total of six phase differences ($\phi_{ij} = \theta_i - \theta_j$ for all $i, j = 1, \dots, 4$). However, if three of them are known, the remaining phase differences can all be expressed as combinations of the three. Generally, for a N -neuron network, only $N - 1$ phase differences are independent. For example, if we choose

$$\phi_{21} = \theta_2 - \theta_1, \tag{1}$$

$$\phi_{31} = \theta_3 - \theta_1, \tag{2}$$

$$\phi_{42} = \theta_4 - \theta_2, \tag{3}$$

where by definition, $\phi_{ij} = -\phi_{ji}$. The other phase differences can be expressed as a combination of the three, e.g., $\phi_{14} = \theta_1 - \theta_4 = -\phi_{41} = -(\phi_{42} + \phi_{21})$. Equations governing the phase differences are

$$\dot{\phi}_{21} = \frac{1}{4} \left[\sum_{j \neq 2} w_{j2} H(\phi_{j2}) - \sum_{j \neq 1} w_{j1} H(\phi_{j1}) \right], \tag{4}$$

$$\dot{\phi}_{31} = \frac{1}{4} \left[\sum_{j \neq 3} w_{j3} H(\phi_{j3}) - \sum_{j \neq 1} w_{j1} H(\phi_{j1}) \right], \tag{5}$$

$$\dot{\phi}_{42} = \frac{1}{4} \sum_{j \neq 4} w_{j4} H(\phi_{j4}) - \sum_{j \neq 2} w_{j2} H(\phi_{j2}), \quad (6)$$

where $H(\phi)$, defined by (13) or (15) in Appendix A, is the phase-resetting function. It is the averaged response in the phase of one neuron to the influence of the other over one oscillation period (Winfree, 1967; Kuramoto, 1984; Ermentrout and Kopell, 1984). It is determined by the coupling between two neurons and the phase response of each in response to the action of the other. $H(\phi)$ is a periodic function with unit period when time is scaled by the period, i.e. $H(\phi) = H(\phi + 1)$. We often express it as the sum of its odd part, $g(\phi) = \frac{1}{2}[H(\phi) - H(-\phi)]$, and its even part, $h(\phi) = \frac{1}{2}[H(\phi) + H(-\phi)]$. The coupling strength is nonnegative, i.e., $w_{ij} \geq 0$. We assume that $w_{ij} = w_{ji}$ for all $i \neq j$ which implies the coupling between each pair of neurons is reciprocal and identical. Since there is no self-coupling, $w_{ii} = 0$ for all i .

The sign of $g'(0)$ determines whether the interaction between two neurons in synchrony is stabilizing or destabilizing since the rate of change in the phase difference between the two is proportional to $-g'(0)$. Thus, $g'(0) > 0$ implies stabilizing interaction while $g'(0) < 0$ is destabilizing. Hansel *et al.* (1995) showed that when synaptic coupling is slow enough, $g'(0) > 0$ when coupling is inhibitory, whereas $g'(0) < 0$ when coupling is excitatory. These results are usually true whenever the synaptic coupling is not instantaneous. Exceptions can occur in type II neurons when the coupling is not slow enough. For simplicity, we here after consider only models in which inhibitory coupling implies $g'(0) > 0$ (stabilizing) and excitatory coupling implies $g'(0) < 0$ (destabilizing) unless indicated otherwise.

Globally uniform distribution of coupling strength is a special case of any heterogeneous distribution and has been studied previously. The triangle distribution in Fig. 1a can not guarantee the existence of phase-clustered states that are model independent. You need to write down the

equations to figure out why this is the case (not shown). We therefore focus on the square distribution in Fig. 1b. This distribution gives rise to several model-independent phase-locked states including the two-cluster state. For this distribution (see Fig.1b), (4)-(6) are simplified to

$$\dot{\phi}_{21} = \frac{1}{4}[w_I(H_{42} - H_{31}) + w_O(H_{12} + H_{32} - H_{21} - H_{41})], \quad (7)$$

$$\dot{\phi}_{31} = \frac{1}{4}[w_I(H_{13} - H_{31}) + w_O(H_{23} + H_{43} - H_{21} - H_{41})], \quad (8)$$

$$\dot{\phi}_{42} = \frac{1}{4}[w_I(H_{24} - H_{42}) + w_O(H_{14} + H_{34} - H_{12} - H_{32})]. \quad (9)$$

Here we used subscripts to simplify the notation for the phase variables in the argument of the H function, namely, $H_{ij} = H(\phi_{ij})$. The Jacobian of this system is

$$J = \frac{w_O}{4} \begin{bmatrix} -H'_{12} - H'_{32} - H'_{21} - H'_{41} & H'_{32} - sH'_{31} & sH'_{42} - H'_{41} \\ H'_{23} + H'_{43} - H'_{21} - H'_{41} & -s(H'_{31} + H'_{13}) - H'_{23} - H'_{43} & H'_{43} - H'_{41} \\ H'_{12} + H'_{32} - H'_{34} - H'_{14} & H'_{34} - H'_{32} & -s(H'_{42} + H'_{24}) - H'_{14} - H'_{34} \end{bmatrix},$$

where $s = w_I/w_O$ is the ratio between the two coupling strengths. Again, subscripts were used to simplify the notation for the arguments of the function H' , i.e., $H'_{ij} = H'(\phi_{ij})$.

Each neuron in the square distribution (Fig. 1b) receives three synaptic inputs, two from its nearest neighbors and one from the diagonal neighbor. Thus, interaction with the diagonal neighbor differs from the interactions with nearest neighbors. If the diagonal coupling is weaker (i.e., $w_I < w_O$), a neuron is more likely to cluster with its diagonal neighbor since the desynchronizing interaction between the two is weaker. The opposite is true if the coupling is inhibitory. Therefore, phase-locked states of (7)-(9) can be classified into two types as a result of this asymmetry. The first is a two-cluster state that is characterized by two synchronized diagonal pairs with a phase difference ψ between the two pairs (Fig. 3a). We call it the state of two in-phase diagonal pairs. The second is called the state of two anti-phase diagonal pairs (Fig. 3b). In this state, each neuron

is anti-phase with its diagonal neighbor.

3.1 Two in-phase diagonal pairs

The state of two in-phase diagonal pairs (Fig. 3a) is characterized by,

$$\phi_{ij} = \begin{cases} 0 & \text{if } i + j \text{ is even,} \\ (-1)^i \psi & \text{if } i + j \text{ is odd.} \end{cases}$$

Substituting this state into (7)-(9), we find that it is a steady-state solution if and only if $g(\psi) = 0$. This condition is identical to the existence of phase-locked states in two coupled oscillators. Thus, there exists a state of two in-phase diagonal pairs for each zero of the function g . Since $g(\psi)$ is the odd part of $H(\psi)$, which depends on both the specifics of the synapse and the neural model, the number of zeros is model dependent. However, $g(\psi) = 0$ is satisfied by all models for $\psi = 0$ and $\frac{1}{2}$ since g is an odd 1-periodic function. Therefore, $\psi = 0$ and $\frac{1}{2}$ are the two model-independent phase-locked states, where $\psi = 0$ is the fully synchronous state and $\psi = \frac{1}{2}$ is the state of two anti-phase clusters. For other ψ values, $g(\psi) = 0$ can be satisfied in some models with carefully chosen synaptic delay. For example, such a solution exists for the model shown in Fig. 9, where $g(\psi) = 0$ for $\psi \approx 0.23$.

Before going through the following results, it is useful to remember that $H'(0) = g'(0)$ and $H'(\frac{1}{2}) = g'(\frac{1}{2})$ (see Appendix). The stability of the state of in-phase diagonal pairs can be determined for all possible values of ψ . Substituting this solution into the Jacobian, we obtain the following eigenvalues $\lambda_1 = -w_O g'(\psi)$, $\lambda_2 = -\frac{w_O}{2}[H'(\psi) + s g'(0)]$, and $\lambda_3 = -\frac{w_O}{2}[H'(-\psi) + s g'(0)]$. Therefore, a necessary condition for stability is $g'(\psi) > 0$. Since ψ is the phase difference between the two clusters, this implies that the out-cluster interaction (between neurons in different clusters)

is stabilizing. To guarantee stability, two more conditions should be satisfied $H'(\psi) + sg'(0) > 0$ and $H'(-\psi) + sg'(0) > 0$. These conditions are satisfied only if at least one of the two terms involved is positive. For excitatory coupling in networks studied here, $g'(0) < 0$. Thus, in-phase or in-cluster interaction (between neurons in each cluster) is destabilizing. Therefore, $H'(-\psi), H'(\psi) > 0$ must be satisfied in order to satisfy the two additional conditions. These conditions are automatically satisfied for some special values of ψ , i.e., 0 and $\frac{1}{2}$ (see next). They also can be satisfied for other values of ψ if $H'(\psi)$ is even (i.e., if $H(\psi)$ is odd). For many current based neuronal models, however, these conditions are not satisfied for $\psi \neq 0, \frac{1}{2}$ since $H'(-\psi)$ and $H'(\psi)$ often have opposite signs.

The fully synchronous state. This is one of the special, model-independent cases of two in-phase diagonal pairs, i.e., $\psi = 0$. Substituting this value into the eigenvalues, we obtain $\lambda_1 = -w_O g'(0)$ and $\lambda_2 = \lambda_3 = -\frac{1}{2}(w_I + w_O)g'(0)$. Thus, the stability is completely determined by $g'(0)$. For excitatory coupling, $g'(0) < 0$. The fully synchronized state is unstable. It is stable for inhibitory coupling since $g'(0) > 0$. This result is in agreement with what we already know. **The state of two anti-phase clusters.** This is the other special case of two in-phase diagonal pairs, i.e., $\psi = \frac{1}{2}$. In this case, we obtain $\lambda_1 = -w_O g'(\frac{1}{2})$ and $\lambda_2 = \lambda_3 = -\frac{w_O}{2}[sg'(0) + g'(\frac{1}{2})] = -\frac{1}{2}[w_I g'(0) + w_O g'(\frac{1}{2})]$. Thus, a necessary condition for stability is $g'(\frac{1}{2}) > 0$. This implies that out-cluster interaction between neurons at anti-phase is stabilizing.

Another condition for stability is $w^* = w_I g'(0) + w_O g'(\frac{1}{2}) > 0$. We call w^* the *total interaction*, which is actually the weighted sum of the values of $g'(\psi)$ at all possible phase differences in a phase-locked state. In the particular state we consider here, neurons are either locked in-phase or out-of-phase. The condition $w^* > 0$ requires the total interaction be stabilizing. For inhibitory coupling,

the in-cluster interaction is stabilizing ($g'(0) > 0$). Thus, the second condition is automatically satisfied if the first is satisfied. Therefore, $g'(\frac{1}{2}) > 0$ is both necessary and sufficient for inhibitory networks. For excitatory coupling, however, $g'(\frac{1}{2}) > 0$ is no longer sufficient. Since now the in-cluster interaction is destabilizing ($g'(0) < 0$), the second condition requires that the stabilizing out-cluster interaction be strong enough to make the total interaction stabilizing. For uniform coupling strength, i.e., $w_O = w_I$, this condition is rarely satisfied because $|g'(0)| \geq |g'(\psi)|$ ($\psi \in [0, 1]$) for most models we checked (see examples in Figs. 5-7). An exceptional example will also be given (see Fig. 9). This explains why robust two-cluster states have rarely been reported in such networks. In networks with heterogeneous coupling strength, $w^* > 0$ can always be satisfied by choosing a small enough ratio between w_I and w_O provided that $g'(\frac{1}{2}) > 0$.

3.2 Two anti-phase diagonal pairs

In the state of two anti-phase diagonal pairs, the phase difference between the two pairs is ψ or $\frac{1}{2} - \psi$ depending on how the difference is defined (see Fig. 3b). Therefore,

$$\phi_{ij} = \begin{cases} \frac{1}{2} & \text{if } i + j \text{ is even,} \\ (-1)^i \psi & \text{if } i, j = 1, 2 \text{ or } 3, 4, \\ (-1)^j (\frac{1}{2} - \psi) & \text{if } i, j = 1, 4 \text{ or } 2, 3. \end{cases}$$

Substituting this state into (7)-(9), we find that it is a solution if and only if $g(\psi) = g(\frac{1}{2} - \psi)$.

Thus, if $g(\psi - \frac{1}{4})$ is an even function (e.g., $g(\psi) = \sin(2\pi\psi)$), then this state is a solution for any ψ between 0 and $\frac{1}{2}$. For $\psi \neq 0, \pm\frac{1}{4}, \frac{1}{2}$, this state is a skewed splay-phase state since the phases are spread but not evenly distributed over one period. Generally, the existence of such a state is model dependent.

For the special values $\psi = 0, \pm\frac{1}{4}, \frac{1}{2}$, $g(\psi) = g(\frac{1}{2} - \psi)$ is satisfied for all models. Therefore, there are four model-independent states. $\psi = 0$ and $\frac{1}{2}$ correspond to two states of two anti-phase clusters. However, they differ from the two-cluster state we previously studied. Here, the diagonal neighbors are anti-phase and the in-phase clusters are formed between nearest neighbors. With uniformly distributed initial phases, it is equally likely for a neuron to form a cluster with its neighbors on the left and on the right. Thus, these two states coexist. Conditions for their existence and stability are identical. For $\psi = \pm\frac{1}{4}$, the four neurons spike alternately at evenly distributed phases over one period. Such a state has previously been called the splay-phase state. The two states corresponding to $\psi = \pm\frac{1}{4}$ coexist and differ only in the order of firing.

The stability of the state of two anti-phase pairs can be determined for all possible values of ψ . Substituting this solution into the Jacobian, we obtain the following eigenvalues: $\lambda_1 = -\frac{w\omega}{2}[g'(\psi) + g'(\frac{1}{2} - \psi)]$, $\lambda_{2,3} = -\frac{w\omega}{4}\{2sg'(\frac{1}{2}) + g'(\psi) + g'(\frac{1}{2} - \psi) \pm \sqrt{[g'(\psi) + g'(\frac{1}{2} - \psi)]^2 - 2[H'(\psi)H'(\frac{1}{2} - \psi) + H'(-\psi)H'(\psi - \frac{1}{2})]}\}$. This allows us to determine the stability of the two model-independent solutions.

The state of two anti-phase clusters. Since the two states for $\psi = 0$ and $\frac{1}{2}$ share the same conditions for existence and stability, we only need to focus on one. Substituting $\psi = 0$ into the eigenvalues given above, we obtain $\lambda_1 = -\frac{w\omega}{2}[g'(0) + g'(\frac{1}{2})]$, $\lambda_2 = -\frac{w\omega}{2}[sg'(\frac{1}{2}) + g'(0)]$, and $\lambda_3 = -\frac{w\omega}{2}(s+1)g'(\frac{1}{2})$. Similar to the two-cluster state of in-phase diagonal pairs, $g'(\frac{1}{2}) > 0$ is a necessary condition for stability. When this condition is satisfied, $\lambda_2 < 0$ can be satisfied by choosing a large enough s value. The last condition to be satisfied is $g'(0) + g'(\frac{1}{2}) > 0$. As pointed out previously, this condition is rarely satisfied for excitatory coupling since $g'(0) < 0$ and often $|g'(0)| > |g'(\frac{1}{2})|$. For inhibitory coupling, however, the necessary condition ($g'(\frac{1}{2}) > 0$) is also

sufficient.

The splay-phase state. There exist two such states corresponding to $\psi = \pm\frac{1}{4}$. The phase difference is $\frac{1}{4}$ between nearest neighbors and is $\frac{1}{2}$ between diagonal neighbors. The phases of the four neurons are evenly distributed over one full period. This is not a phase-clustered state since no neuron is in synchrony with any other neuron. Thus, there is no “in-cluster” interaction, implying that $g'(0)$ which determines the interaction between in-phase neurons will not appear in stability conditions. The eigenvalues for these states are: $\lambda_1 = -w_O g'(\frac{1}{4})$, $\lambda_{2,3} = -\frac{w_O}{2}[s g'(\frac{1}{2}) + g'(\frac{1}{4}) \pm i h'(\frac{1}{4})]$. λ_2 and λ_3 are a pair of complex conjugates with a real part $Re\{\lambda_{2,3}\} = -\frac{1}{2}[w_I g'(\frac{1}{2}) + w_O g'(\frac{1}{4})]$. Therefore, a necessary condition for the stability of this state is $g'(\frac{1}{4}) > 0$. Again, this condition ensures that the interaction between neurons at a phase difference of $\frac{1}{4}$ is stabilizing. However, this is not enough to guarantee the stability. The second condition to satisfy is $w^* = w_I g'(\frac{1}{2}) + w_O g'(\frac{1}{4}) > 0$. This means that the total interaction, w^* , should also be stabilizing. When the necessary condition is satisfied, this can be achieved irrespective of the sign of $g'(\frac{1}{2})$, i.e., the interaction between anti-phase neurons can be either stabilizing ($g'(\frac{1}{2}) > 0$) or destabilizing ($g'(\frac{1}{2}) < 0$). In the latter case, $w^* > 0$ implies $w_O |g'(\frac{1}{4})| > w_I |g'(\frac{1}{2})|$, i.e., the stabilizing interaction should be stronger than the destabilizing one.

3.3 Other possible phase-locked states

We mainly focus on phase-clustered states that involve more than one cluster with more than one neuron in each cluster. We have studied all possible two-cluster states in the four-neuron network in Fig. 1b. In addition, we also studied the fully synchronous state and the splay-phase state. All these states are model independent. However, there still may exist other phase-locked

states that we have ignored. The existence of those states is usually model or circuit dependent, requiring either some special properties of the model or some special choices of coupling strengths. For example, we did not discuss another type of solutions in which two nearest neighbors form anti-phase pairs. The existence of this type of states depends on special choices of w_O and w_I . However, these conditions are easy to satisfy. Under these conditions, skewed splay-phase state can be stable (not shown). However, this does not give any new phase-clustered state.

4 Clustered states in a network of six neurons

To demonstrate the stability of clustered states with more than two clusters, we study a network of six neurons. In a six-neuron network, there are multiple choices of coupling strength distribution with enough symmetry to generate clustered states. We do not study all possible distributions but will focus on two (Fig. 4) that most likely yield phase-clustered states. Fig. 4(a1) shows a distribution with two triplets, one containing odd-numbered neurons and the other containing the even numbered neurons. This symmetry feature can be seen in the dotted lines representing a coupling strength w_I between neurons in each triplet (Fig. 4(a1)). The solid lines connecting neurons in different triplets represent a coupling strength w_O . We call it the triplet distribution. Fig. 4(b1) shows a distribution in which the three diagonal pairs are coupled with a strength w_I (dotted lines) and all other coupling strengths are w_O (solid lines). This divides the neurons into three diagonal doublets. Thus, we call it the doublet distribution.

The reduced phase description of this network is given by (12) in Appendix A for $N = 6$. Since we are interested only in the phase differences, for six neurons, there are five independent phase differences. The choice of the phase difference variables can make the analysis much simpler, but

this choice depends on the distribution of coupling strength.

4.1 The triplet distribution

For the 5 independent phase differences in this distribution, we pick one phase difference between the two triplets, $\phi_{21} = \theta_2 - \theta_1$, and two phase differences within each triplet making up the four remaining phase differences, $\phi_{31} = \theta_3 - \theta_1$, $\phi_{53} = \theta_5 - \theta_3$, $\phi_{42} = \theta_4 - \theta_2$, and $\phi_{64} = \theta_6 - \theta_4$. All other phase differences can be expressed as a combination of these five differences. Equations for these phase difference variables and the corresponding Jacobian matrix are given in the Appendix by (16)-(20) and (21), respectively.

Phase-locked solutions reflecting the symmetry features of the triplet distribution can be classified into two types: two in-phase triplets (Fig. 4(a2)) and two splay-phase triplets (Fig. 4(a3)).

The state of two in-phase triplets. This state is described by the following phase differences (Fig. 4(a2)),

$$\phi_{ij} = \begin{cases} 0 & \text{if } i + j \text{ is even,} \\ (-1)^i \psi & \text{if } i + j \text{ is odd.} \end{cases}$$

Substituting these phase differences into (16)-(20), we find that it is a steady-state solution if and only if $g(\psi) = 0$. This condition is identical to that for the state of two in-phase pairs in the four-neuron network.

Substituting this state into the Jacobian and solving for the eigenvalues, we obtain $\lambda_1 = -w_O g'(\psi)$ and $\lambda_{2,4} = -\frac{w_O}{2} [H'(\psi) + s g'(0)]$, and $\lambda_{3,5} = -\frac{w_O}{2} [H'(-\psi) + s g'(0)]$. These eigenvalues again are identical to those for the state of two in-phase diagonal pairs in the four-neuron network.

This suggests that conditions for the existence and stability of the state of two clusters with

identical in-cluster coupling strength might be independent of the size of the network. Again, only two such states are model independent. One is for $\psi = 0$ which is the fully synchronous state. The other is for $\psi = \frac{1}{2}$ which is a two-cluster state. The stability conditions for these two states are identical to those for the corresponding states in the four-neuron network given in the previous Section.

The state of two splay-phase triplets. This state is characterized by (see Fig. 4(a3))

$$\phi_{ij} = \begin{cases} (-1)^i \psi & \text{if } i, j = 1, 2, \text{ or } 3, 4, \text{ or } 5, 6, \\ (-1)^j (\frac{1}{3} - \psi) & \text{if } i, j = 2, 3, \text{ or } 4, 5, \text{ or } 6, 1, \\ (-1)^i (\frac{1}{3} + \psi) & \text{if } i, j = 1, 4, \text{ or } 3, 6, \text{ or } 5, 2. \end{cases}$$

Substituting these phase differences into (16)-(20), we find that this state is a steady-state solution if and only if $g(\psi) = g(\frac{1}{3} - \psi) - g(\frac{1}{3} + \psi)$. To study the stability, we can substitute this solution into the Jacobian and determine the eigenvalues. There is always one real eigenvalue: $\lambda_1 = -\frac{w\omega}{3}[g'(\psi) + g'(\frac{1}{3} - \psi) + g'(\frac{1}{3} + \psi)]$. Although analytical expressions of other eigenvalues can be obtained generally, they are too complicated for any practical use. Therefore, we only focus on the special, model-independent states of this type. These include six states for $\psi = \frac{l}{6}$, $l = 1, 2, \dots, 6$. When l is even, $\psi = \frac{l}{6}$ corresponds to a state of three clusters with evenly distributed phases and with two neurons in each cluster (Fig. 4(a3)). The three three-cluster states corresponding to $l = 2, 4, 6$ coexist and share identical stability conditions. The difference is the combination of the two neurons in each cluster. An odd-numbered neuron can be in synchrony with any one of the even-numbered neurons. The eigenvalues for these states are: $\lambda_1 = -\frac{w\omega}{3}[2g'(\frac{1}{3}) + g'(0)]$, $\lambda_{2,3} = -(s+1)\frac{w\omega}{6}[3g'(\frac{1}{3}) \pm i\sqrt{3}h'(\frac{1}{3})]$, and $\lambda_{4,5} = -\frac{w\omega}{6}[2g'(0) + (1+3s)g'(\frac{1}{3}) \pm i(1-s)\sqrt{3}h'(\frac{1}{3})]$, where $h'(\phi) = \frac{1}{2}[H'(\phi) - H'(-\phi)]$ is the derivative of the even part of function H . Thus, $g'(\frac{1}{3}) > 0$ is

a necessary condition. If this condition is satisfied, $2g'(0) + (1 + 3s)g'(\frac{1}{3}) > 0$ can be satisfied by choosing a large enough value of s . The condition that turns out problematic for many models of excitatory networks is $2g'(\frac{1}{3}) + g'(0) > 0$ since $g'(0) < 0$ and often $|g'(0)| > 2|g'(\frac{1}{3})|$.

When l is odd, the state corresponding to $\psi = \frac{l}{6}$ is a splay-phase state. There exist three such states for $l = 1, 3, 5$, all sharing the same conditions for existence and stability. They only differ in the order of spiking of each neuron in each cycle. The eigenvalues for these states are: $\lambda_1 = -\frac{w\omega}{3}[2g'(\frac{1}{6}) + g'(\frac{1}{2})]$, $\lambda_{2,3} = -\frac{w\omega}{6}[3g'(\frac{1}{6}) + 3sg'(\frac{1}{3}) \pm i\sqrt{3}(h'(\frac{1}{6}) - sh'(\frac{1}{3}))]$, and $\lambda_{4,5} = -\frac{w\omega}{6}[2g'(\frac{1}{2}) + 3sg'(\frac{1}{3}) + g'(\frac{1}{6}) \pm i\sqrt{3}(h'(\frac{1}{6}) + sh'(\frac{1}{3}))]$. Since these conditions do not involve $g'(0)$, they are not difficult to satisfy. We found that non-uniform coupling strength is not necessary for the stability of these states in the models we studied.

4.2 The doublet distribution

As shown in Fig. 4(b1), neurons in this distribution are divided into three diagonal doublets. We pick two phase differences between neurons in different doublets $\phi_{21} = \theta_2 - \theta_1$ and $\phi_{31} = \theta_3 - \theta_1$, and three phase differences between neurons within each doublet $\phi_{41} = \theta_4 - \theta_1$, $\phi_{52} = \theta_5 - \theta_2$, $\phi_{63} = \theta_6 - \theta_3$. Equations for these variables are given in eqs.(22)-(26), and the corresponding Jacobian is given by eq.(27).

Based on the symmetry features, we also can classify the possible solutions into two types: three in-phase doublets (Fig. 4(b2)) and three anti-phase doublets (Fig. 4(b3)). When restricted to model-independent solutions only, the phases of the three in-phase doublets and of the three anti-phase doublets should be evenly distributed on the unit circle as shown in Figs. 4(b2-b3).

The state of three in-phase doublets. This state (see Fig. 4(b2)) is characterized by

$$\phi_{ij} = \begin{cases} 0 & \text{if } |i - j| = 3, \\ \pm \frac{1}{3} & \text{if } i - j = \pm 1, \mp 2, \pm 4, \mp 5. \end{cases}$$

Note that there are two such states coexist since by changing the relative order of spiking of the doublets, we got another state that is equivalent.

Substituting this state into eqs.(22)-(26), we confirm this is a steady-state solution. For stability, we substitute this state into the Jacobian and obtain the following eigenvalues: $\lambda_{1,2} = -w_O g'(\frac{1}{3}) \pm i \frac{w_O}{\sqrt{3}} h'(\frac{1}{3})$ and $\lambda_{3,4,5} = -\frac{1}{3}[w_I g'(0) + 2w_O g'(\frac{1}{3})]$, where the relationship $g'(\frac{1}{3}) = g'(\frac{2}{3})$ was used. Again, a necessary condition for stability of this clustered state is $g'(\frac{1}{3}) > 0$. A second condition is $sg'(0) + 2g'(\frac{1}{3}) > 0$ which requires that the total interaction be stabilizing. For an inhibitory network, this condition is satisfied whenever the necessary condition is satisfied. For an excitatory network, however, this condition can be satisfied when the ratio between the coupling strengths s is small.

The state of three anti-phase doublets. This state (see Fig. 4(b3)) is model-independent for two special cases. In one case, all doublets are in synchrony yielding two anti-phase clusters of three neurons each. This state coexists with three other equivalent states since each neuron can be in synchrony with the other two doublets in two different ways, i.e. four different combinations. In the other case, phases of the three doublets are evenly distributed over one period. This is the splay-phase state of the six-neuron network. Eight such states coexist since the neurons can spike in 8 different orders.

For the two-cluster states, we focus on the one shown in Fig. 4(b3)

$$\phi_{ij} = \begin{cases} 0 & \text{if } i + j \text{ is even,} \\ \frac{1}{2} & \text{if } i + j \text{ is odd.} \end{cases}$$

By solving the eigenvalues of the Jacobian at this state, we obtain $\lambda_1 = -\frac{w\Omega}{3}(2 + s)g'(\frac{1}{2})$, and $\lambda_{2,3} = -\frac{w\Omega}{6}[3g'(0) + (1 + 2s)g'(\frac{1}{2})]$, and $\lambda_{4,5} = -\frac{w\Omega}{2}[g'(0) + g'(\frac{1}{2})]$. Similar to the two-cluster state in the four-neuron network and in the triplet distribution of the six-neuron network, $g'(\frac{1}{2}) > 0$ is necessary. However, among the other two conditions the condition $g'(0) + g'(\frac{1}{2}) > 0$ is usually not satisfied in most models with excitatory coupling.

For the splay-phase states, we focus on the one that is shown in Fig. 4(b3)

$$\phi_{ij} = \begin{cases} \frac{1}{2} & \text{if } |i - j| = 3, \\ \pm\frac{1}{3} & \text{if } i - j = \pm 1, \mp 2, \\ \pm\frac{1}{6} & \text{if } i - j = \mp 4, \pm 5. \end{cases}$$

By solving the eigenvalues of the corresponding Jacobian, we obtain $\lambda_{1,2} = -\frac{w\Omega}{2}[g'(\frac{1}{6}) + g'(\frac{1}{3})] \pm i\sqrt{3}\frac{w\Omega}{2}[h'(\frac{1}{6}) - h'(\frac{1}{3})]$, $\lambda_3 = -\frac{w\Omega}{3}[2g'(\frac{1}{6}) + sg'(\frac{1}{2})]$, $\lambda_{4,5} = -\frac{w\Omega}{6}[g'(\frac{1}{6}) + 3g'(\frac{1}{3}) + 2sg'(\frac{1}{2})] \pm i\sqrt{3}\frac{w\Omega}{6}[h'(\frac{1}{6}) + h'(\frac{1}{3})]$. Note that the real part of all the eigenvalues contains only values of $g'(\phi)$ at the existing phase differences: $\phi = \frac{1}{6}, \frac{1}{3}, \frac{1}{2}$.

5 Numerical results

Phase description is only approximate, working better for relatively weak coupling and quick relaxation of the perturbed back on to the orbit. The phase theory is totally deterministic and does not take into account the effects of noise. Also, other model-dependent phase-locking states may coexist with the states predicted by the theory. It is therefore sensible to show that the

theory applies satisfactorily to a wide variety of realistic and theoretical models. To confirm the stability conditions derived in previous sections, we carried out numerical studies of clustered states in four-neuron and six-neuron networks. We used three different neuronal models including the integrate-and-fire (IF) model, the Wang-Buzsáki (WB) model (Wang and Buzsáki, 1998) and the Hodgkin-Huxley (HH) model. Detailed descriptions of the model equations, coupling terms, and parameter values are given in Appendix B. Stability conditions derived in previous sections apply to networks of both excitatory and inhibitory neurons. However, we focus here on networks of excitatory neurons since robust phase-clustered states have rarely been reported in such networks.

5.1 Two-cluster states in four-neuron networks

The analysis in Section 3 showed that there are two different types of anti-phase two-cluster states: one with in-phase diagonal pairs and one with anti-phase diagonal pairs. In both cases, $g'(\frac{1}{2}) > 0$ is a necessary condition. A second condition for stability is different for the two cases. When the diagonal pairs are anti-phase, this condition is $g'(0) + g'(\frac{1}{2}) > 0$, but becomes $sg'(0) + g'(\frac{1}{2}) > 0$ ($s = w_I/w_O$) when the diagonal pairs are in-phase. The two conditions are identical when $s = 1$, i.e., when the coupling is uniform. For inhibitory coupling, stability is guaranteed if $g'(\frac{1}{2}) > 0$ since $g'(0) > 0$. Note that in this case, the two-cluster state always coexists with the stable, fully synchronous state. For excitatory coupling, however, the stability of the state of two anti-phase clusters is not guaranteed by $g'(\frac{1}{2}) > 0$ since $g'(0) < 0$. The key is the relative magnitudes of $|g'(0)|$ and $g'(\frac{1}{2})$. In most known models including the ones we used in this study, $|g'(0)| > g'(\frac{1}{2})$. Thus, the total interaction cannot be stabilizing for $s \geq 1$. This is why clustered states were rarely found in networks with uniform excitatory coupling. This also is why, in the square distribution of

the four-neuron network, the states of two synchronous clusters involving two anti-phase diagonal pairs usually are unstable. However, when s is much smaller than 1, the stability condition ($sg'(0) + g'(\frac{1}{2}) > 0$) for the state of two synchronous diagonal pairs can be satisfied. This is because when s is small, the destabilizing in-cluster interaction is much weaker than the stabilizing out-cluster interaction. Fig. 5 shows such a case for a four-neuron network of IF models in square distribution. Synaptic coupling is modeled by an alpha function with a fixed time constant $\tau = 0.4$. For the parameter values used in our simulations, the odd part of the phase-resetting function $g(\phi)$ (dotted curve) and its derivative $g'(\phi)$ (solid curve) were calculated (see Fig. 5a). We found that $g'(0) = -0.287$ and $g'(\frac{1}{2}) = 0.0855$. Thus, the necessary condition is satisfied. However, the two-cluster state with anti-phase diagonal pairs is unstable since $g'(0) + g'(\frac{1}{2}) < 0$. With a choice of $w_O = 0.02$ and $w_I = 0.004$ (i.e. $s = 0.2$), the second condition for the stability of the two-cluster state with in-phase diagonal pairs, $w^*/w_O = sg'(0) + g'(\frac{1}{2}) = 0.0281 > 0$, also is satisfied. Numerical simulations confirmed the existence of the two-cluster state involving synchronized diagonal pairs in this model. It was obtained for several different initial conditions in the presence of noise with an intensity $D = 0.02$, including fully synchronous initial phase (Fig. 5b) and several random initial phase distributions. See Fig. 5c for the case of one specific choice of random initial phase distribution. As we shall demonstrate later (Fig. 10), this state actually coexists with a stable splay-phase state but the latter is obtained only for more restricted initial conditions.

The IF model is the simplest and most abstract model used in the study of synchrony. The phase of an IF neuron is always advanced by an excitatory input. Such a phase-response property is called type I (Hansel et al, 1995). Some other current-based, biophysical models, including the WB model, exhibit a similar property. Fig. 6 shows the occurrence of a two-cluster state in a

four-neuron network of WB models. The coupling is synaptic with a slow time scale (see Appendix B for details). According to Fig. 6a, $g'(0) = -5.143$ and $g'(\frac{1}{2}) = 2.126$. Similar to the network of IF models, only the two-cluster state with synchronous diagonal pairs can be stable. With the choice of $w_O = 0.01$ and $w_I = 0.002$ (i.e., $s = 0.2$), $w^*/w_O = sg'(0) + g'(\frac{1}{2}) = 1.1 > 0$ is satisfied. Numerical simulations confirmed the existence of this two-cluster state (Fig. 6b-d). We obtained this state with different initial phase distributions, including the fully synchronous (Fig. 6b) and random distributions (Fig. 6c). Independent noise with an intensity $D = 0.01 \mu A/cm^2$ was present in all simulations.

As an example of current-based models with a phase-response property of type II, the HH model was used in our simulations. The phase of a type II neuron can be delayed or advanced depending on the timing of the stimulus. Our results are independent of the type of neuron in the network. For the parameter values used in our simulations, $g'(0) = -1.2747$ and $g'(\frac{1}{2}) = 0.2702$. Thus, for a four-neuron network of HH neurons (Fig. 7), the only stable two-cluster state is the one in which the two diagonal pairs are in synchrony. With the choice of $w_O = 0.01$ and $w_I = 0.002$ ($s = 0.2$), $w^*/w_O = sg'(0) + g'(\frac{1}{2}) = 0.01526 > 0$, thereby satisfying the stability conditions. Numerical simulations confirmed the existence of this stable two-cluster state (see Fig. 7).

5.2 Clustered states in six-neuron networks

Results in Section 4 showed both the two-cluster and three-cluster states can exist in the six-neuron network. The necessary condition, $g'(\frac{1}{2}) > 0$, for the two-cluster state is identical for both the doublet and triplet distributions. However, the additional conditions are different, $g'(0) + g'(\frac{1}{2}) > 0$ for the doublet distribution and $sg'(0) + g'(\frac{1}{2}) > 0$ for the triplet distribution. The condition

$g'(0) + g'(\frac{1}{2}) > 0$ is rarely satisfied with excitatory coupling by most models, thus the two-cluster state in the doublet distribution is usually unstable. The condition $sg'(0) + g'(\frac{1}{2}) > 0$ can be satisfied for sufficiently small s in most models, and this condition is identical to the second stability condition for the state of two synchronous diagonal pairs in the four-neuron network. Under the same conditions as in Figs. 5-7, we were able to obtain stable two-cluster states in six-neuron networks of the three models in the triplet distribution of coupling strengths (not shown).

Stability conditions for the three-cluster state are $g'(\frac{1}{3}) > 0$ along with $sg'(0) + 2g'(\frac{1}{3}) > 0$ for the doublet distribution and $g'(0) + 2g'(\frac{1}{3}) > 0$ for the triplet distribution. When the original parameter values of the WB model were used, we obtain $g'(0) = -5.143$, $g'(\frac{1}{3}) = 1.6113$, and $g'(\frac{1}{2}) = 2.126$ (see Fig. 6a). Thus, the three-cluster state is not stable in the triplet distribution since $g'(0) + 2g'(\frac{1}{3}) < 0$. With the choice of $s = w_I/w_O = 0.2$ (i.e., w_O is 5 times w_I), we find that stability conditions for the two-cluster state in the triplet distribution and the three-cluster state in the doublet distribution can both be satisfied. Therefore, the clustered state we can obtain is determined by the distribution of coupling strengths. Numerical simulations confirmed that, for the initial phase distributions tested, the two-cluster state occurred (Fig. 8a,b) with triplet distribution (Fig. 4(a1)) and the three-cluster state was obtained (Fig. 8c,d) with doublet distribution (Fig. 4(b1)).

We carried out simulations in a network of six IF models under similar conditions and confirmed the predictions of the analysis. Simulations also were carried out in a network of six HH model neurons. By changing the rise time of the synaptic gating from $\tau = 12$ to $\tau = 5$, we obtained a $g'(\phi)$ function that is shown in Fig. 9a. Since now $g'(\frac{1}{2}) < 0$, the two-cluster state is unstable. However, $g'(0) = -2.078$, $g'(\frac{1}{3}) = 2.892$, which indicates that $|g'(\frac{1}{3})| > |g'(0)|$. Therefore, the

stability of the three-cluster state is satisfied even when s is 1 or even slightly larger than 1 (see Fig. 9b,c). This is an example showing that although nonuniform distribution of coupling strength facilitates the stability of clustered states, it is not a necessity. For some models with a special choice of synaptic delay (e.g., the one in Fig. 9a), $|g'(0)|$ is not necessarily the global maximum of the function $g'(\phi)$. However, for most known models with original parameter values, $|g'(0)|$ is the global maximum of the $g'(\phi)$ function. This explains why stable clustered states were rarely found in networks of these model neurons with uniform, excitatory coupling.

6 Co-existence of multiple states

Although the networks studied here are small, co-existence of multiple states is common. The fully synchronous state is always a solution irrespective of the neuronal model and the distribution of coupling strengths. This solution usually coexists with other solutions. For example, in the square distribution of the four-neuron network, the fully synchronous state co-exists with at least two other types of states: the two-cluster state and the splay-phase state. The latter includes two equivalent, coexisting states. Also, there exist three two-cluster states of which two are equivalent. Thus, for a network of four neurons, there exist a total of six model-independent states, one fully synchronous state, three clustered states, and two splay-phase states. The number of coexisting states can increase if we take into account other possible states whose existence is model or coupling-strength dependent.

Fig. 10 shows all the coexisting, model-independent states in the square distribution of a network of four IF neurons with excitatory coupling. In order to separate all the distinct states, we used the average phase difference, $\bar{\phi} = \frac{1}{3}(\phi_{21} + \phi_{31} + \phi_{42})$, as the bifurcation variable. Thus,

$\bar{\phi} = 0$ for the fully synchronous state (FS), $\bar{\phi} = \frac{1}{6}$ for the two-cluster state of synchronous diagonal pairs (SDP), $\bar{\phi} = \frac{1}{3}, \frac{1}{2}$ for the two two-cluster states of anti-phase diagonal pairs (ADP₁, ADP₂), and $\bar{\phi} = \frac{5}{12}, \frac{7}{12}$ for the two splay-phase states (SP₁, SP₂).

By applying the stability conditions derived in Section 3 to this network with excitatory coupling, we found that FS and ADP are always unstable (dotted lines). The SDP is stable only for smaller values of s , and the two SP states are always stable. Fig. 10b shows the s -dependent eigenvalues of the SDP and SP states, λ_{SDP} and λ_{SP} , respectively. The eigenvalue λ_{SP} remains negative for all positive values of s , however, the value of λ_{SDP} is negative for smaller values of s , then increases linearly, as a function of s , to positive values. This is related to the fact that excitatory coupling destabilizes synchrony between two neurons in each cluster. Thus, the stability of SDP is favored by weaker in-cluster coupling (i.e., smaller w_I) and stronger out-cluster coupling (i.e., larger w_O) resulting in a smaller value of $s = w_I/w_O$. For the parameter values used here, the critical value of s is about 0.3. In other words, an out-cluster coupling strength that is about 3 times the in-cluster coupling strength is sufficient to maintain the stability of this two-cluster state. Numerical simulations indicate that when SDP and SP states were both stable (i.e., $s < 0.3$), the SDP state was reached with most random initial phase distributions. Furthermore, when the network was initiated in the SP state, increasing the intensity of noise for a finite period of time usually destroyed the SP state and led to the occurrence of the SDP state (see Fig. 10c). These results suggest that the SDP state has a larger attraction basin than the SP state.

7 Summary and Discussion

In the present study, we extended the analysis of two weakly coupled oscillators to networks of four and six neurons. Based on the theory of reduced phase description, we studied the steady-state solutions to the equations of independent phase-differences that are phase-locked states of the network. Due to the small size of the networks, we were able to derive conditions for the existence and stability of clustered states in these networks. The existence and stability of model-independent clustered states strongly depend on the symmetry in the distribution of coupling strengths. Higher degree of symmetry leads to the coexistence of more phase-locked states. However, the stability of clustered states is favored by asymmetric distributions in networks of excitatory neurons.

The analysis shows that synchrony in the form of phase clustering is possible in networks of all-to-all coupled excitatory neurons when the synaptic coupling is slow. It provides for the first time an explanation for the lack of numerical studies showing the existence of stable clustered states in networks of excitatory neurons. Furthermore, conditions that are both necessary and sufficient for the occurrence of stable clustered states are derived and numerical studies presented to confirm these results. Conditions that are sufficient but not necessary for the stability of a variety of phase-locked solutions were previously obtained by Chow (1998). The reason for why mutually desynchronizing neurons can stay synchronized in each cluster is that neurons in other clusters force them to stay synchronized. Therefore, a necessary condition for the stability of clustered states in excitatory networks is that out-cluster interactions must be stabilizing and strong enough to overcome the in-cluster desynchronizing interactions.

At most of the phase-locked states studied here, interaction between neurons is determined by the sign and the magnitude of the slope of the odd part of the phase-resetting function, $g'(\psi)$.

For example, $g'(0)$ characterizes the interaction between neurons at zero phase difference. Thus, the sign of $g'(0)$ determines whether the interaction between synchronized neurons is stabilizing or destabilizing. Similarly, the sign of $g'(\frac{1}{2})$ determines if the interaction between neurons at anti-phase is stabilizing. For neurons coupled through excitatory synapses, $g'(0) < 0$, which means the in-phase interaction is destabilizing. Therefore, the fully synchronized state is unstable in this network. However, a state of two synchronized clusters at anti-phase can be stable if $g'(\frac{1}{2}) > 0$ which means the anti-phase interaction is stabilizing. This occurs when the anti-phase interaction is sufficiently strong to keep neurons in each cluster stay synchronized. But in most model neurons studied so far, $|g'(0)| > |g'(\frac{1}{2})|$, i.e., the magnitude of the in-phase interaction is larger than that of the anti-phase interaction (for an exception, see Fig. 9). Therefore, the stability conditions are easier to satisfy if the coupling strength becomes nonuniform selectively as to strengthen the stabilizing out-cluster interaction and/or weaken the destabilizing in-cluster interaction.

An important question arises as whether these results on small networks can be extended to large networks. The answer is positive but several new problems arise in the study of large networks. First, the analysis is no longer as straightforward and more technical. Second, there are a larger number of possible distributions of coupling strengths and a larger number of possible co-existing states. Third, clustered states with a large number of clusters can occur in large networks, contrary to networks of four and six neurons that can generate clustered states of only two or three clusters. Thus, the stability conditions become more complicated and difficult to understand intuitively. For example, the analysis in this paper shows that a necessary condition for the stability of a state of two anti-phase clusters is $g'(\frac{1}{2}) > 0$. Similarly, $g'(\frac{1}{3}) > 0$ is a necessary condition for the stability of a state of three clusters at evenly distributed phase differences. Based

on these results, it is tempting to conjecture that for a state of n splay-phase clusters, a necessary condition is $g'(\frac{1}{n}) > 0$. A reason for this conjecture is that $\frac{1}{n}$ is the basic out-cluster phase difference in the state of n splay-phase clusters. It seems natural to assume that $g'(\frac{1}{n})$ should be stabilizing if the overall out-cluster interaction is stabilizing. However, this conjecture is not true for $n > 4$. This is because when the number of clusters increases, it is no longer necessary for all possible out-cluster interactions be stabilizing. The sufficient condition given by Chow (1998) actually requires that all out-cluster interactions be stabilizing. In a stable multi-cluster state, some out-cluster interactions can even be destabilizing provided that the combined, overall out-cluster interaction remains stabilizing. For these reasons, we are preparing a separate manuscript for the results on large networks. Another direction to extend the results in the paper is to include a mixture of excitatory and inhibitory neurons in a network. For example, the network in hippocampus that generates gamma rhythms has been shown to involve both excitatory and inhibitory neurons (Whittington *et al.*, 1997; Kopell *et al.*, 2000). The analysis for networks with mixed types of synapses can be done within the same theoretical framework if the combined synaptic interaction remains weak. In this case, the definition of the phase-resetting function should take into account the sum of all types of synaptic interactions.

Phased-locked states in a network of coupled oscillators have been studied extensively in models of animal gaits (Collins and Stewart, 1993; Golubitsky *et al.*, 1998; 1999). These authors used the theory of symmetric Hopf bifurcation to derive general conditions that guarantee the existence of bifurcations from the trivial stationary solution to periodic solutions with prescribed spatio-temporal symmetries. All model-independent states we studied here have been shown to exist in their models for quadruped locomotion. These states are referred to as primary gaits and occur as a

result of symmetries in the network. For example, the FS state corresponds to pronk, the SP states correspond to walk, the SDP state relates to trot, and the ADP states are related to either pace or bound. One important result of their analysis is that the eight-cell network is the smallest possible network that can produce all primary gaits without unwanted conjugacies (conjugate solutions are identical under symmetry permutations of the neurons). In particular, conjugacy between pace and trot seems to contradict with observations in virtually all quadrupeds. However, in our network of four identical neurons, trot (SDP) and pace (SP) are dynamically independent, but not pace and bound. Note that coupling in our four-neuron network is all-to-all while their networks contain nearest-neighbor coupling only. Furthermore, our analysis provides conditions for both the existence and stability, thus the concept of *dynamical independence* in our study includes both conditions. Actually, all primary gaits generated by our four-neuron network coexist in the same parameter region (see Fig. 10). However, our analysis shows that this minimal network is still capable of making only one of them stable selectively (e.g. walk). Our results further demonstrate that even when two stable gaits (e.g. walk and trot) coexist, one of them (trot) is predominant since it has a larger attraction basin. Switching between a stable gait (walk) to another stable gait (trot) only requires changing the ratio between the two coupling strengths in our model. If both excitatory and inhibitory synapses are allowed between each pair (project under investigation), it is likely that this network can produce one gait at a time that is both stable and predominant.

Our analysis provides explicit functional dependence of the eigenvalues that determine the stability of clustered states on the coupling strengths. This opens the door to understanding how changes in the relative magnitudes of coupling strengths induce changes in the synchrony state of a network. This makes it possible to construct a network of current-based, realistic neuronal

models that can perform similar computational tasks as those performed by Hopfield's networks (Hopfield, 1984). Results presented here can also be applied to the study of synchrony in realistic neural networks in which excitatory synapses play a dominant role.

A Phase reduction of weakly coupled oscillators

The phase equations

All neurons in our networks are identical, and each is described by a system of differential equations.

$$\frac{d\mathbf{X}}{dt} = \mathbf{F}(\mathbf{X}), \quad (10)$$

For a current-based, biophysical model, $\mathbf{X} = (V, q_1, \dots, q_{n_v-1})$, is a vector of n_v variables, including the membrane potential V and $n_v - 1$ gating variables. \mathbf{F} is a nonlinear vector field that characterizes the dynamics of the neuron. Assuming that there exists a stable T -periodic solution $\mathbf{X}_s(t)$, thus $\mathbf{X}_s(t + T) = \mathbf{X}_s(t)$. In the vicinity of this periodic orbit, a phase variable ϕ can be defined (Winfree, 1967; Kuramoto, 1984) that uniquely determines the states of the neuron. Changes in the phase by perturbations in different variables at different time can be determined by the adjoint $\mathbf{Z}(\psi)$ (see e.g. Keener and Sneyd, 1998) of the periodic solution. The function was originally called the “sensitivity function” (Winfree, 1967) and is often called the “phase-response function”. For a current-based model, only the equation for V is directly perturbed by synaptic currents. Thus, only the first component of the vector $\mathbf{Z}(\psi)$, $Z_1(\psi)$, is nonzero.

For a network of N identical neurons with identical, all-to-all synaptic coupling, the dynamics is governed by

$$\frac{d\mathbf{X}_i}{dt} = \mathbf{F}(\mathbf{X}_i) + \frac{1}{N} \sum_{j \neq i} w_{ji} \mathbf{S}(\mathbf{X}_j, \mathbf{X}_i), \quad (11)$$

where $i, j = 1, \dots, N$, $w_{ji} = w_{ij}$ for symmetric coupling, and \mathbf{S} characterizes the synaptic interaction between two neurons. Only the first component of \mathbf{S} , S_1 , is nonzero since the gating variables are not influenced by coupling directly.

When the coupling is weak (i.e., $w_{ji} \ll 1$ for all i, j), this network can be described approximately by the following system of phase equations:

$$\frac{d\theta_i}{dt} = \frac{1}{N} \sum_{j \neq i} w_{ji} H(\theta_j - \theta_i), \quad (12)$$

where $\theta_i = t + \psi_i$ ($i = 1, 2, \dots, N$) is the relative phase variable and the phase-resetting function $H(\theta_j - \theta_i)$ is defined by

$$H(\theta_j - \theta_i) = \frac{1}{T} \int_0^T \mathbf{Z}(\mathbf{t} + \theta_i) \cdot \mathbf{S}(t + \theta_j, t + \theta_i) dt = \frac{1}{T} \int_0^T Z_1(\tau) S_1(\tau + \theta_j - \theta_i, \tau) d\tau. \quad (13)$$

H is T -periodic since Z_1 and S_1 are T -periodic. For simplicity, we scale the time and the phase variables by the period T so the period is always 1; thus $H(\phi) = H(\phi + 1)$. We split the H -function into an odd part and an even part, $H(\phi) = g(\phi) + h(\phi)$, where $g(\phi) = \frac{1}{2}(H(\phi) - H(-\phi))$ and $h(\phi) = \frac{1}{2}(H(\phi) + H(-\phi))$. Note that $g(0) = g(\frac{1}{2}) = h'(0) = h'(\frac{1}{2}) = 0$ since they are odd, continuous, periodic functions. Note also $H'(0) = g'(0)$ and $H'(\frac{1}{2}) = g'(\frac{1}{2})$. The function H characterizes the averaged response in the phase of one oscillator to the influence of the other over one oscillation period (see Kuramoto, 1984; Ermentrout and Kopell, 1984). Thus, the phase-resetting function is determined by the coupling between two oscillators and the phase variation of each in response to the action of the other.

A similar theory has been developed (Van Vreeswijk et al, 1994) for the integrate-and-fire (IF) model. In this case, $\mathbf{X} = X$ is a scalar and $\mathbf{F}(\mathbf{X}) = X_0 - X$, where X_0 is a constant. The periodic orbit is obtained by resetting the value of X to 0 whenever it reaches 1. The relative phase for the i th neuron can be defined by $\theta_i = \omega \int_0^{X_i} \frac{ds}{X_0 - s} - \omega t = -\omega \ln(\frac{X_0 - X_i}{X_0}) - \omega t$, where $T = \frac{1}{\omega} = \int_0^1 \frac{ds}{X_0 - s} = \ln(\frac{X_0}{X_0 - 1})$.

In terms of these new phase variables, a network of IF neurons coupled by an alpha function

can be expressed as

$$\frac{d\theta_i}{dt} = F(\omega t + \theta_i) \sum_{j \neq i} \frac{w_{ji}}{N} E_T(\omega t + \theta_j) \quad (14)$$

where $F(\omega t + \theta_i) = \frac{\omega}{X_0} e^{\frac{1}{\omega}(\omega t + \theta_i)}$ and $E_T(\theta) = \sum_{l=-\infty}^0 A_\tau((\theta - l)T)$. Here, A_τ is the alpha function defined by $A_\tau(t) = \text{Heav}(t)\tau^{-2}te^{-t/\tau}$.

When the coupling is weak, i.e. $|\sum_{j \neq i} w_{ji} E_{ji}(t)| \ll |X_0 - X_i|$, the system can be reduced to a system of coupled phase equations that is identical to that given by eq.(12) in which

$$H(\theta_j - \theta_i) = \frac{1}{T} \int_0^T d\tau F(\omega\tau - (\theta_j - \theta_i)) E_T(\omega\tau) = \int_0^1 ds F(s - (\theta_j - \theta_i)) E_T(s). \quad (15)$$

Phase difference equations for the six-neuron network

The triplet distribution. The equations governing the phase differences, ϕ_{21} , ϕ_{31} , ϕ_{42} , ϕ_{53} , and ϕ_{64} , are

$$\dot{\phi}_{21} = \frac{w_I}{6}(H_{42} + H_{62} - H_{31} - H_{51}) + \frac{w_O}{6}(H_{12} + H_{32} + H_{52} - H_{21} - H_{41} - H_{61}), \quad (16)$$

$$\dot{\phi}_{31} = \frac{w_I}{6}(H_{13} + H_{53} - H_{31} - H_{51}) + \frac{w_O}{6}(H_{23} + H_{43} + H_{63} - H_{21} - H_{41} - H_{61}), \quad (17)$$

$$\dot{\phi}_{42} = \frac{w_I}{6}(H_{24} + H_{64} - H_{42} - H_{62}) + \frac{w_O}{6}(H_{14} + H_{34} + H_{54} - H_{12} - H_{32} - H_{52}), \quad (18)$$

$$\dot{\phi}_{53} = \frac{w_I}{6}(H_{15} + H_{35} - H_{13} - H_{53}) + \frac{w_O}{6}(H_{25} + H_{45} + H_{65} - H_{23} - H_{43} - H_{63}), \quad (19)$$

$$\dot{\phi}_{64} = \frac{w_I}{6}(H_{26} + H_{46} - H_{24} - H_{64}) + \frac{w_O}{6}(H_{16} + H_{36} + H_{56} - H_{14} - H_{34} - H_{54}). \quad (20)$$

The Jacobian matrix of this system is $w_O J$ where J is given by

$$\frac{w_O}{6} \begin{bmatrix} -O_2 - E_1 & (3+5)_2 - s(3+5)_1 & s(4+6)_2 - (4+6)_1 & H'_{52} - sH'_{51} & sH'_{62} - H'_{61} \\ E_{(3-1)} & -E_3 - 2sg'_{31} - sH'_{51} & (4)_{(3-1)} + (6)_{(3-1)} & s(5)_{(3-1)} & (6)_{(3-1)} \\ -O_{(4-2)} & (3)_{(4-2)} + (5)_{(4-2)} & -O_4 - 2sg'_{42} - sH'_{62} & (5)_{(4-2)} & s(6)_{(4-2)} \\ E_{(5-3)} & -s(1)_{(5-3)} - E_{(5-3)} & (4)_{(5-3)} + (6)_{(5-3)} & -E_5 - s2g'_{53} - sH'_{15} & (6)_{(5-3)} \\ -O_{(6-4)} & (3)_{(6-4)} + (5)_{(6-4)} & -s(2)_{(6-4)} - O_{(6-4)} & (5)_{(6-4)} & -O_6 - 2sg'_{64} - sH'_{26} \end{bmatrix}. \quad (21)$$

where $s = w_I/w_O$, $g'_{ij} = g'(\phi_{ij})$, $(i+j)_l = H'_{il} + H'_{jl}$, $(l)_{(i-j)} = H'_{li} - H'_{lj}$, $O_i = \sum_{l \text{ odd}} H'_{li}$,

$E_i = \sum_{l \text{ even}} H'_{li}$, and $E_{l-k} = E_l - E_k$, $O_{l-k} = O_l - O_k$. Recall that $H'_{ij} = H'(\phi_{ij})$.

The doublet distribution. The equations governing the phase differences, ϕ_{21} , ϕ_{31} , ϕ_{41} , ϕ_{52} , and ϕ_{63} , are

$$\dot{\phi}_{21} = \frac{w_I}{6}(H_{52} - H_{41}) + \frac{w_O}{6}(H_{12} + H_{32} + H_{42} + H_{62} - H_{21} - H_{31} - H_{51} - H_{61}), \quad (22)$$

$$\dot{\phi}_{31} = \frac{w_I}{6}(H_{63} - H_{41}) + \frac{w_O}{6}(H_{13} + H_{23} + H_{43} + H_{53} - H_{21} - H_{31} - H_{51} - H_{61}), \quad (23)$$

$$\dot{\phi}_{41} = \frac{w_I}{6}(H_{14} - H_{41}) + \frac{w_O}{6}(H_{24} + H_{34} + H_{54} + H_{64} - H_{21} - H_{31} - H_{51} - H_{61}), \quad (24)$$

$$\dot{\phi}_{52} = \frac{w_I}{6}(H_{25} - H_{52}) + \frac{w_O}{6}(H_{15} + H_{35} + H_{45} + H_{65} - H_{12} - H_{32} - H_{42} - H_{62}), \quad (25)$$

$$\dot{\phi}_{63} = \frac{w_I}{6}(H_{36} - H_{63}) + \frac{w_O}{6}(H_{16} + H_{26} + H_{46} + H_{56} - H_{13} - H_{23} - H_{43} - H_{53}). \quad (26)$$

The Jacobian of this system can be calculated to give

$$\frac{w_O}{6} \begin{bmatrix} -B_2^{(5+2)_1} & (6+3)_{(2-1)} & H'_{42} - sH'_{41} & sH'_{52} - H'_{51} & (6)_{(2-1)} \\ (5+2)_{(3-1)} & -B_3^{(6+3)_1} & H'_{43} - sH'_{41} & H'_{53} - H'_{52} & sH'_{63} - H'_{61} \\ (5+2)_{(4-1)} & (6+3)_{(4-1)} & -2sg'_{41} - A_4^{(4,1)} & (5)_{(4-1)} & (6)_{(4-1)} \\ -A_5^{(5,2)} + A_2^{(5,2)} & (6+3)_{(5-2)} & (4)_{(5-2)} & -2sg'_{52} - A_5^{(5,2)} & (6)_{(5-2)} \\ (5+2)_{(6-3)} & -A_6^{(6,3)} + A_3^{(6,3)} & (4)_{(6-3)} & (5)_{(6-3)} & -2sg'_{63} - A_6^{(6,3)} \end{bmatrix}. \quad (27)$$

where again $s = w_I/w_O$, $g'_{ij} = g'(\phi_{ij})$, $(l)_{(i-j)} = H'_{li} - H'_{lj}$, $(l+k)_{i-j} = (l)_{(i-j)} + (k)_{(i-j)} = (l)_i - (l)_j + (k)_i - (k)_j$, $A_j^{(l,k)} = \sum_{q \neq l,k} H'_{qj}$, and $B_j^{(l+k)_i} = H'_{li} + H'_{ki} + A_j^{(l,k)}$.

B Models, coupling terms, and numerical methods

The Integrate-and-Fire Model

The network of N integrate-and-fire model neurons is described by $dX_i/dt = X_0 - X_i + I_{syn}^i$ where X_i ($i = 1, 2, \dots, N$) is the state variable of the i th neuron and $X_0 = 1.3$. Synaptic coupling is modeled by $I_{syn}^i = \frac{1}{N} \sum_{j=1}^N w_{ji} \int_0^\infty \alpha(s, \tau) S_j(t-s) ds$, where $\alpha(s, \tau) = (s/\tau^2) \exp(-s/\tau)$ is the alpha function with a time constant τ , and $S_j(t) = \sum_k \delta(t - t_k)$ is the output spike train from the j th neuron firing at times t_k . w_{ji} is the coupling strength between the i th and j th neuron.

The Wang-Buzsáki Model

The network of N Wang-Buzsáki model neurons is described by

$$C_m \frac{dV_i}{dt} = I_{app} - g_{Na} m_\infty^3 h(V_i - V_{Na}) - g_K n^4 (V_i - V_K) - g_L (V_i - V_L) - I_{syn}^i, \quad (28)$$

where V_i ($i = 1, 2, \dots, N$) is the membrane potential of the i th neurons. $m_\infty = \alpha_m / (\alpha_m + \beta_m)$ with $\alpha_m = -0.1(V_i + 35) / [\exp(-0.1(V_i + 35)) - 1]$ and $\beta_m = 4\exp(-(V_i + 60)/18)$. The gating variable q ($q = h$ and n) is governed by $dq/dt = \phi[\alpha_q(1 - q) - \beta_q q]$ with $\alpha_h = 0.07\exp(-(V_i + 58)/20)$, $\beta_h = 1 / [\exp(-0.1(V_i + 28)) + 1]$, $\alpha_n = -0.01(V_i + 34) / [\exp(-0.1(V_i + 34)) - 1]$, and $\beta_n = 0.125\exp(-(V_i + 44)/80)$.

Synaptic currents received by the i th neuron is modeled by, $I_{syn}^i = \sum_{j \neq i} g_{ji} s_j (V_i - V_{syn})$, where g_{ji} are the synaptic conductances. For excitatory coupling, $V_{syn} = 100$ mV. Synaptic gating is described by $ds_j/dt = \alpha F(V_j)(1 - s_j) - \beta s_j$, where $F(V_j) = \frac{1}{1 + \exp(-V_j/2)}$, $\alpha = 12$ msec⁻¹ and $\beta = 0.1$ msec⁻¹.

Other parameter values are $C_m = 1$ μ F/cm², $g_{Na} = 35$ mS/cm², $V_{Na} = 55$ mV, $g_K = 35$ mS/cm², $V_K = -90$ mV, $g_L = 0.1$ mS/cm², $V_L = -65$ mV, $\phi = 5$. $I_{app} = 1.0$ μ A/cm².

The Hodgkin-Huxley Model

The Hodgkin-Huxley model we used is described by

$$C_m \frac{dV_i}{dt} = I_{app} - g_{Na} m^3 h (V_i - V_{Na}) - g_K n^4 (V_i - V_K) - g_L (V_i - V_L) - I_{syn}^i \quad (29)$$

with the gating variable q , $q = m, h, n$, described by $\frac{dq}{dt} = \alpha_q(1 - q) - \beta_q q$ where $\alpha_m = \frac{0.1(V_i + 40)}{1 - \exp((-V_i - 40)/10)}$, $\beta_m = 4\exp((-V_i - 65)/18)$; $\alpha_n = \frac{0.01(V_i + 55)}{1 - \exp((-V_i - 55)/10)}$, $\beta_n = 0.125\exp((-V_i - 65)/80)$; and $\alpha_h = 0.07\exp((-V_i - 65)/20)$, $\beta_h = \frac{1}{1 + \exp((-V_i - 35)/10)}$. The parameter values are: $C_m = 1$ μ F/cm², $V_{Na} = 50$ mV, $V_K = -77$ mV, $V_L = -54.4$ mV, $g_{Na} = 120$ mS/cm², $g_K = 36$ mS/cm², $g_L = 0.3$ mS/cm², and $I_{app} = 10.0$ μ A/cm².

The synaptic current received by the i th neuron is given by

$$I_{syn}^i = \sum_{j \neq i} g_{ji} (V_i - V_{syn}) \int_0^\infty (s/\tau^2) \exp(-s/\tau) S_j(t - s) ds \text{ where } S_j(t) = \sum_k \delta(t - t_k) \text{ represents the}$$

output spike train from the j th neuron firing at times t_k . g_{ji} are the synaptic conductances. For excitatory coupling, $V_{syn} = 100 \text{ mV}$.

Numerical methods

We used the fourth-order Runge-Kutta method with fixed step sizes, 0.001 for the IF model and 0.01 ms for the WB and HH models. To ensure the robustness of the clustered states obtained, we added a small, independent noise term, $\sqrt{2D}\eta(t)$, to each neuron at each time step. Here $\eta(t)$ is an independent Gaussian white noise with $\langle \eta(t + \tau)\eta(t) \rangle = \delta(\tau)$. The magnitude D is small in all the simulations (see figure legends).

References

- [1] Abbott LF (1994) Decoding neuronal firing and modeling neural networks. *Quarterly Review of Biophysics* 27:291-331.
- [2] Chow, CC (1998) Phase-locking in weakly heterogeneous neural networks. *Physica D* 118:343–370.
- [3] Collins JJ, Stewart IN (1993) Coupled nonlinear oscillators and the symmetries of animal gaits. *J. Nonlinear Sci.* 3:349-392.
- [4] Ermentrout, B, Kopell N (1984) Frequency plateaus in a chain of weakly coupled oscillators. *SIAM J. Math. Anal.* 15:215–237.
- [5] Ernst U, Pawelzik K, Geisel T (1998) Delay-induced multistable synchronization of biological oscillators. *Phys. Rev. E* 57:2150–2162.
- [6] Glass L, Mackey MC (1988) *From Clocks to Chaos. The Rhythm of Life*. Princeton University Press, New Jersey.
- [7] Golomb D, Hansel D, Shraiman B, Sompolinsky H (1992) Clustering in globally coupled phase oscillators. *Phys. Rev. A* 45:3516–3530.
- [8] Golomb D, Rinzel J (1994) Clustering in globally coupled inhibitory neurons. *Physica D* 72:259-282.
- [9] Golomb D, Wang XJ, Rinzel J (1994) Synchronization properties of spindle oscillations in a thalamic reticular nucleus. *J. Neurophysiol.* 72:1109–1126.

- [10] Golubitsky M, Steward I, Buono P-L, Collins JJ (1998) A modular network for legged locomotion. *Physica D* 115:56-72.
- [11] Golubitsky M, Steward I, Buono P-L, Collins JJ (1999) Symmetry in locomotor central pattern generators and animal gaits. *Nature* 401:693-695.
- [12] Gray CM, Konig P, Engel AK, Singer W (1989) Oscillatory responses in cat visual cortex exhibit inter-columnar synchronization which reflects global stimulus properties. *Nature* 338:334-337.
- [13] Gray CM (1994) Synchronous oscillations in neuronal systems: mechanisms and functions. *J. Comput. Neurosci.* 1:11-38.
- [14] Grillner, S (1975) Locomotion in vertebrates: central mechanisms and reflex interaction. *Physiol. Rev.* 55:247-392.
- [15] Gutnick MJ, Connors BW, Prince DA (1982) Mechanisms of neocortical epileptogenesis in vitro. *J. Neurophysiol.* 48:1321-1335.
- [16] Hansel D, Mato G, Neunier C. (1995) Synchrony in excitatory neural networks. *Neural Comp.* 7:307-337.
- [17] Hopfield, JJ (1984) Neurons with Graded Response Have Collective Computational Properties Like Those of Two-state Neurons, *Proc. Natl. Acad. Sci. USA* 81:3088-2092.
- [18] Keener J, Sneyd J. (1998) *Mathematical Physiology*. Springer, New York.
- [19] Knobil E (1987) A hypothalamic pulse generator governs mammalian reproduction. *News Physiol. Sci.* 2:42-43.

- [20] Kopell N, Ermentrout GB, Whittington MA, Traub RD (2000) Gamma rhythms and beta rhythms have different synchronization properties. *Proc. natl. Acad. Sci. USA* 97:1867–1872.
- [21] Kuramoto, Y (1984) *Chemical Oscillations, Waves and Turbulence*. Springer, New York.
- [22] Leng G (1988) *Pulsatility in Neuroendocrine Systems*. CRC Press, Boca Raton, Florida.
- [23] Lytton WW, Sejnowski TJ (1991) Simulations of cortical pyramidal neurons synchronized by inhibitory interneurons. *J. Neurophysiol.* 66:1059–1079.
- [24] Mirollo, RE, Strogatz, SH (1990) Synchronization of pulse-coupled biological oscillators. *SIAM J. Math. Anal.* 50:1645–1662.
- [25] Nichols S, Wiesenfeld K (1992) Ubiquitous neutral stability of splay-phase states. *Phys. Rev. A* 45:8430–8435.
- [26] Nicolelis MA, Baccala LA, Lin RC, Chapin JK (1995) Sensorimotor encoding by synchronous neural ensemble activity at multiple levels of the somatosensory system. *Science* 268:1353–1358.
- [27] Prechtl JC, Cohen LB, Pesaran B, Mitra PP, Kleinfeld D (1997) Visual stimuli induce waves of electrical activity in turtle cortex. *Proc. natl. Acad. Sci. USA* 94:7621–7626.
- [28] Reikling JC, Feldman JL (1998) PreBotzinger complex and pacemaker neurons: hypothesized site and kernel for respiratory rhythm generation. *Ann. Rev. Physiol.* 60:385–405.
- [29] Sherman, A, Rinzel J (1992) Rhythmogenic effects of weak electrotonic coupling in neural models. *Proc. natl. Acad. Sci. USA* 89:2471–2474.

- [30] Sortie DW, Rand RH (1986) Dynamics of two strongly coupled relaxation oscillators. *SIAM J. Math. Anal.* 46:56–67.
- [31] Smith JC, Ellenberger HH, Ballanyi K, Richter DW, Feldman JL (1991) Pre-Botzinger complex: a brainstem region that may generate respiratory rhythm in mammals. *Science* 254:726–729.
- [32] Steriade M, McCormick DA, Sejnowski TJ (1993) Thalamocortical oscillations in the sleeping and aroused brain. *Science* 262:679–685.
- [33] Traub, RD, Jeffreys, JGR, Whittington, MA (1999) *Fast Oscillations in Cortical Circuits*. MIT Press, Cambridge.
- [34] Van Vreeswijk C, Abbott LF, Ermentrout, B (1994) When inhibition not excitation synchronizes neural firing. *J. Comput. Neurosci.* 1:313-321.
- [35] Van Vreeswijk C (1996) Partial synchronization in populations of pulse coupled oscillators. *Phys. Rev. E* 54:5522–5537.
- [36] Wang XJ, Rinzel J (1992) Alternating and synchronous rhythms in reciprocally inhibitory model neurons. *Neural Comp.* 4:84–97.
- [37] Wang XJ, Buzsaki G (1996) Gamma oscillation by synaptic inhibition in a hippocampal interneuronal network model. *J. Neurosci.* 16:6402-6413.
- [38] Wang YQ, Wang ZD, Li YX, Pei X (2000) Synchronous phase clustering in a network of neurons with spatially decaying excitatory coupling. Submitted.

- [39] Whittington MA, Traub RD, Faulkner HJ, Stanford IM, Jefferys JG (1997) Recurrent excitatory postsynaptic potentials induced by synchronized fast cortical oscillations. *Proc. natl. Acad. Sci. USA* 94:12198-121203.
- [40] Williams TL, Sigvardt KA, Kopell N, Ermentrout GB, Remler M (1990) Forcing of coupled nonlinear oscillators: Studies of intersegmental coordination in the lamprey locomotor central pattern generator. *J. Neurophysiol.* 64:862–871.
- [41] Winfree, A (1967) Biological Rhythms and the behavior of populations of coupled oscillators. *J. Theor. Biol.* 16:15–42.

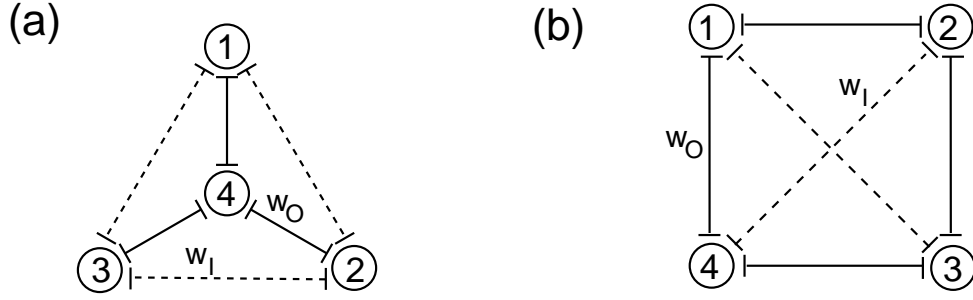


Figure 1: Two heterogeneous distributions of coupling strength in a spatially distributed four-neuron network. Each neuron is denoted by a numbered-circle. Synaptic coupling is reciprocal and identical between any two neurons and therefore is represented by a single line. Coupling strength is assumed to decrease as distance increases. (a) The triangle distribution. (b) The square distribution.

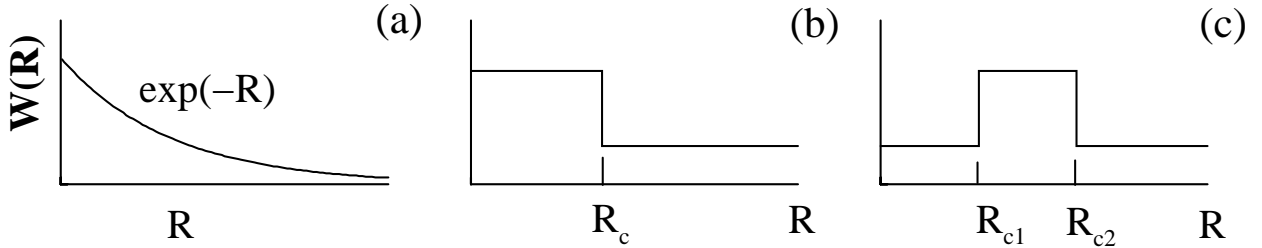


Figure 2: Possible distributions of coupling strength as a function of radial distance. (a) Exponential decay. (b) Centered with cut-off distance R_c . (c) Off-centered with on- and off-distances R_{c1} and R_{c2} respectively.

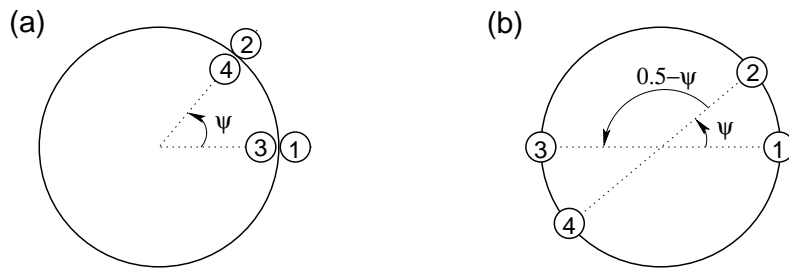


Figure 3: Two types of phase-locked states in the four-neuron network. The big circle represents the phase-space of the phase model. (a) Two in-phase diagonal pairs at a phase difference ψ . $\psi = 0$ and $1/2$ are, respectively, the in-phase one-cluster state and the anti-phase two-cluster state. (b) Two anti-phase diagonal pairs at a phase difference ψ . $\psi = 0$ and $\frac{1}{2}$ correspond to states of two anti-phase clusters. $\psi = \pm\frac{1}{4}$ represent two splay-phase states.

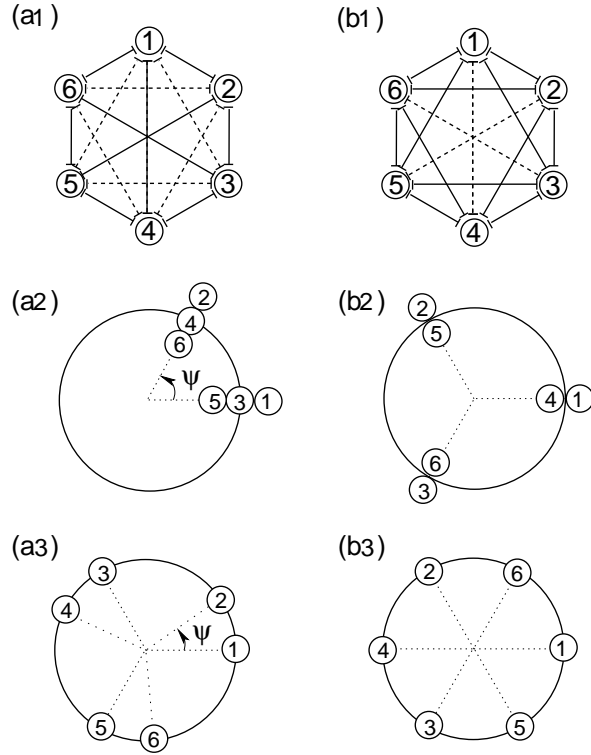


Figure 4: Two distributions of coupling strength in a six-neuron network and phase-space representations of possible solutions. (a1-a3) The triplet distribution and the two corresponding types of phase-locked states. (b1-b3) The doublet distribution and the two corresponding types of phase-locked states. Neurons are represented by numbered circles and coupling strengths are denoted by dashed lines (for w_I) and solid lines (for w_O).

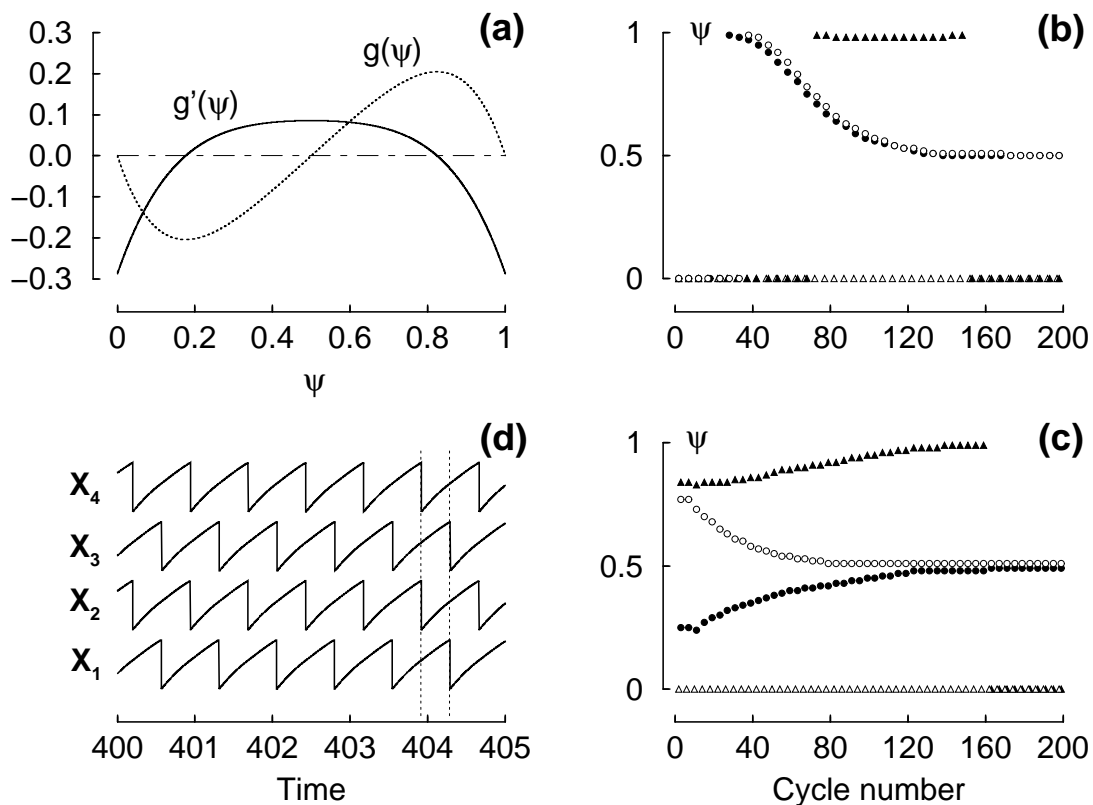


Figure 5: Two-cluster state in a net (Fig. 1b) of four excitatory integrate-and-fire neurons. Coupling is modeled by an alpha function with a time constant $\tau = 0.4$. The coupling strengths used are $w_O = 0.02$ and $w_I = 0.004$. (a) The odd part of the phase-resetting function, $g(\psi)$ (dotted), and its derivative, $g'(\psi)$ (solid). To plot the two with the same vertical scale, $g(\phi)$ was multiplied by 10. (b) and (c) Stroboscopic graphs showing the spiking times of each neuron during each oscillation cycle relative to that of a pre-selected reference neuron (open triangles). To avoid crowding in data points, four cycles were skipped for each data presented. The initial phase distribution was fully synchronized in (b) and was random in (c). (d) Time series of the membrane potential of the 4 neurons after a transient of 400 time units. The two dotted lines indicate that diagonal neighbors are synchronized.

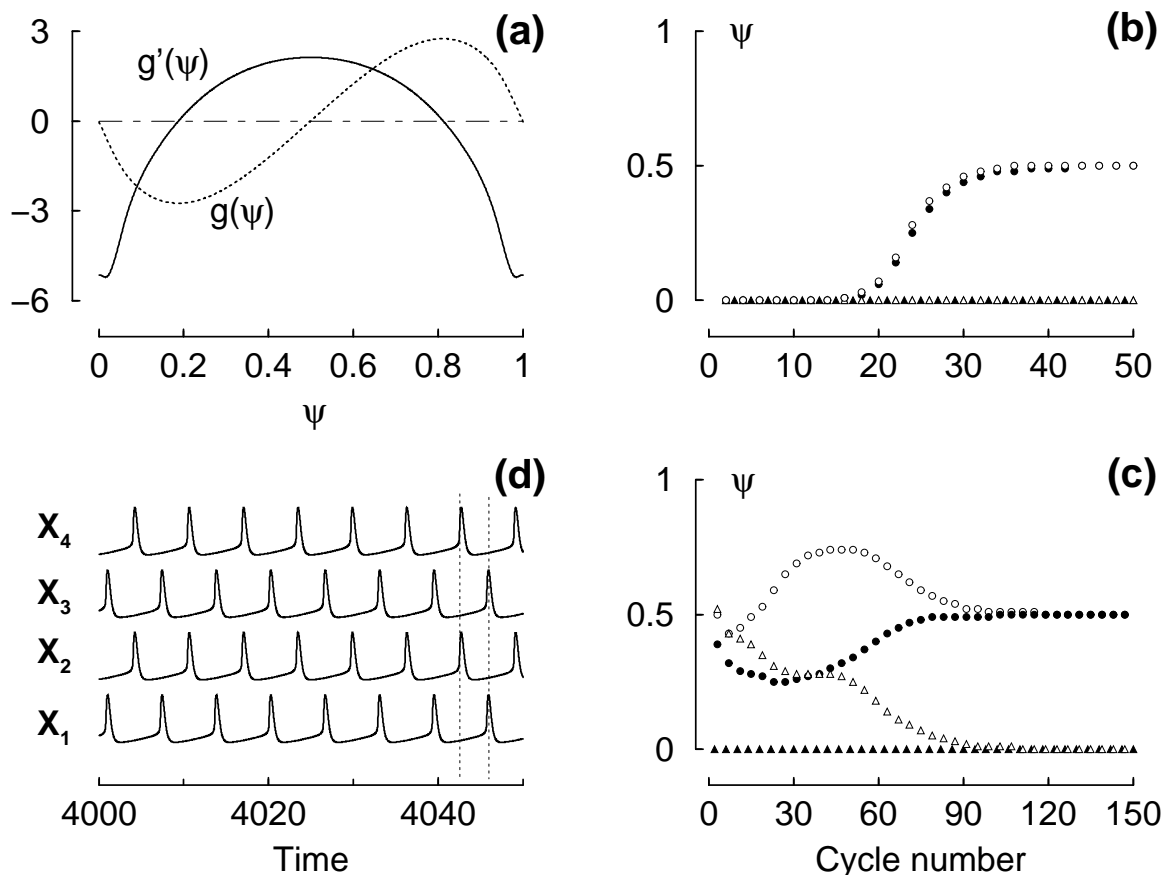


Figure 6: Two-cluster state in a network (Fig. 1b) of four excitatory Wang-Buzsáki neurons. The coupling strengths used are $w_O = 0.01 \mu A/cm^2$ and $w_I = 0.002 \mu A/cm^2$. The on and off rates of the synaptic gating are $\alpha = 12 msec^{-1}$ and $\beta = 0.1 msec^{-1}$, respectively. (a) The odd part of the phase-resetting function, $g(\phi)$ (dotted line), and its derivative $g'(\phi)$ (solid line). (b) and (c) Stroboscopic pictures of the relative spiking times of the four neurons for synchronized and random initial phase distributions, respectively. (d) The time series of the membrane potentials of the 4 neurons. The vertical, dotted lines show that diagonal neighbors become synchronized eventually.

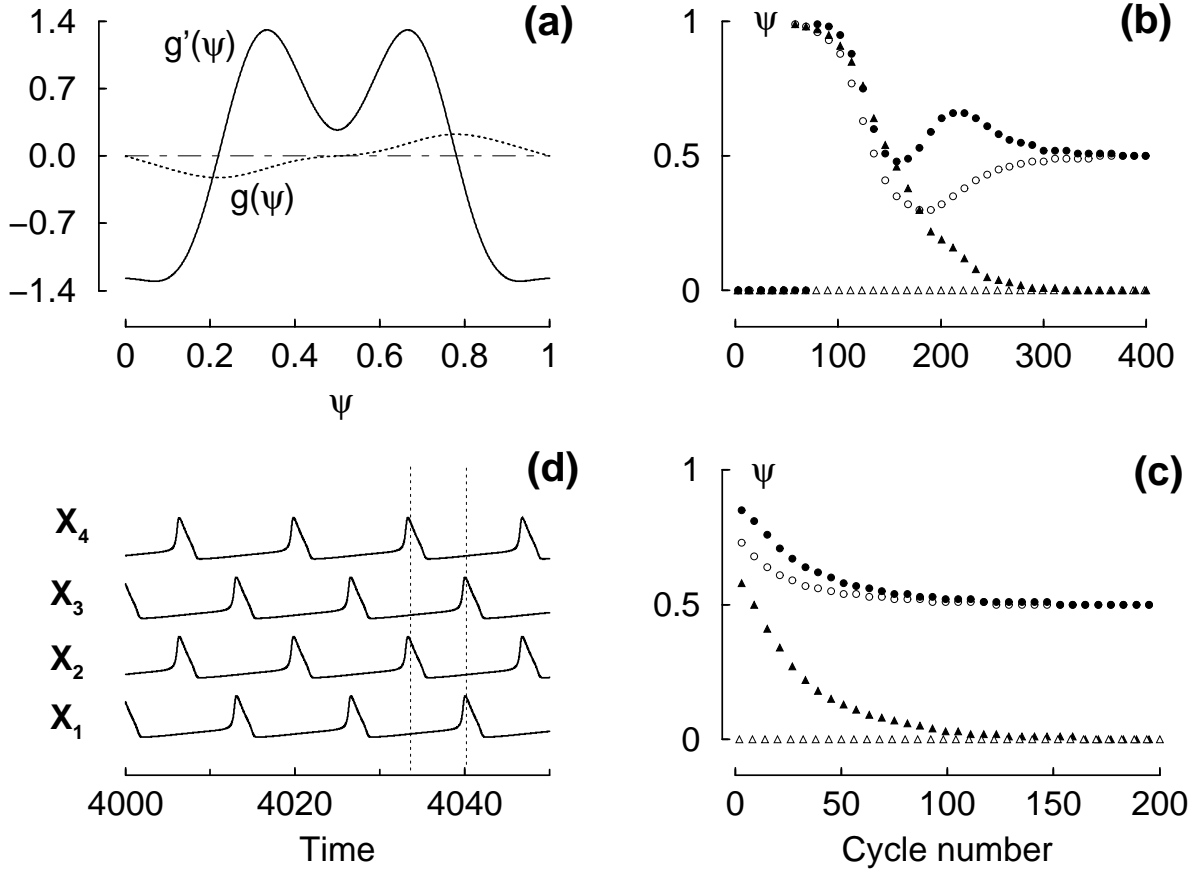


Figure 7: Two-cluster state in a network of four excitatory Hodgkin-Huxley neurons. The synaptic gating is described by an alpha function with a time constant $\tau = 12 \text{ msec}$. The coupling strengths used are $w_O = 0.1 \mu\text{A}/\text{cm}^2$ and $w_I = 0.01 \mu\text{A}/\text{cm}^2$. (a) $g(\phi)$ (dotted line) and $g'(\phi)$ (solid line). (b) and (c) Stroboscopic pictures of the time evolution of the relative phases. The initial phase distribution was fully synchronous in (b) and random in (c). (d) The time series of the membrane potentials of the four neurons.

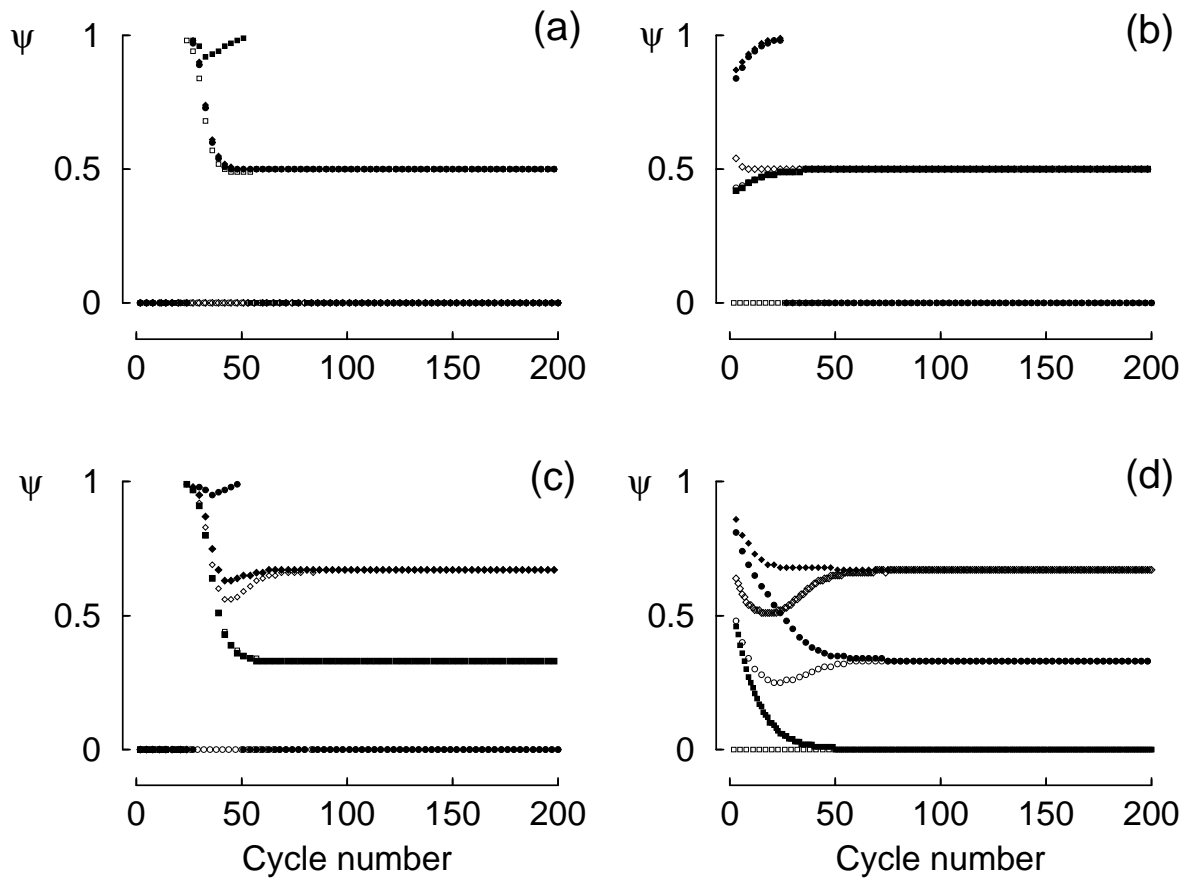


Figure 8: Clustered states in a network of six Wang-Buzsáki model neurons with excitatory synaptic coupling. Parameter values are the same as in Fig. 6. Stroboscopic pictures of the time evolution of the phases: (a) and (b) for the triplet distribution (Fig. 4(a1)), (c) and (d) for the doublet distribution (Fig. 4(b1)). The initial phase distribution was fully synchronous in (a) and (c) but was random in (b) and (d). It shows that changing the distribution of coupling strengths from the triplet to the doublet distribution can switch the firing pattern of the network from a two-cluster to a three-cluster state.

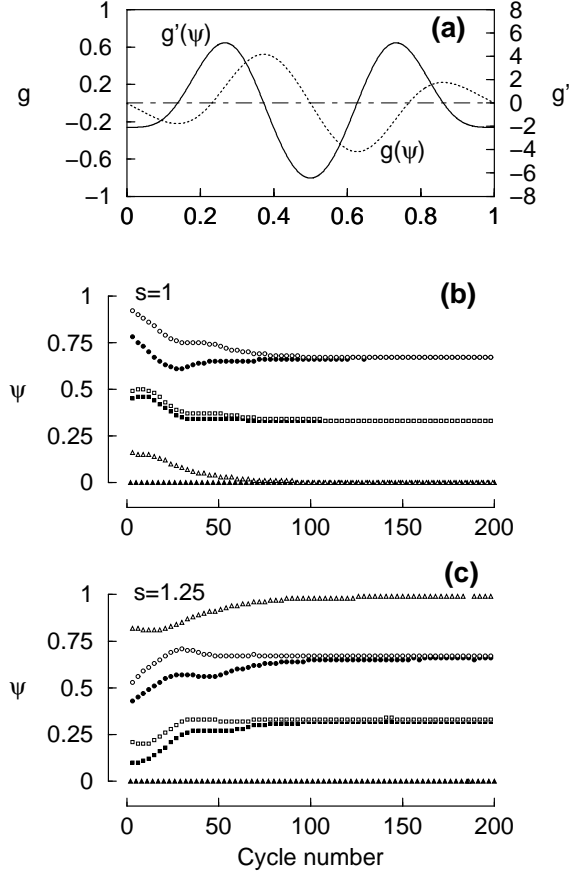


Figure 9: Clustered states in a network of six excitatory Hodgkin-Huxley neurons with a special phase-resetting function. (a) $g(\phi)$ (dotted) and $g'(\phi)$ (solid). Note that for the specific choice of $\tau = 5 \text{ msec.}$, $|g'(\frac{1}{3})| > |g'(0)|$. (b) and (c) Stroboscopic pictures of the time evolution of the phases with random initial phase distributions. In (b), the coupling strength is uniformly distributed, $w_O = w_I = 0.02 \mu A/cm^2$ (i.e., $s = 1$). In (c), the heterogeneity in the coupling strength strengthens the destabilizing in-cluster interactions, $w_O = 0.02$, $w_I = 0.025 \mu A/cm^2$ (i.e., $s = 1.25$). But it is not enough to destabilize the clustered state since $|g'(\frac{1}{3})| > 1.25|g'(0)|$. Other parameters values are the same as in Fig. 7.

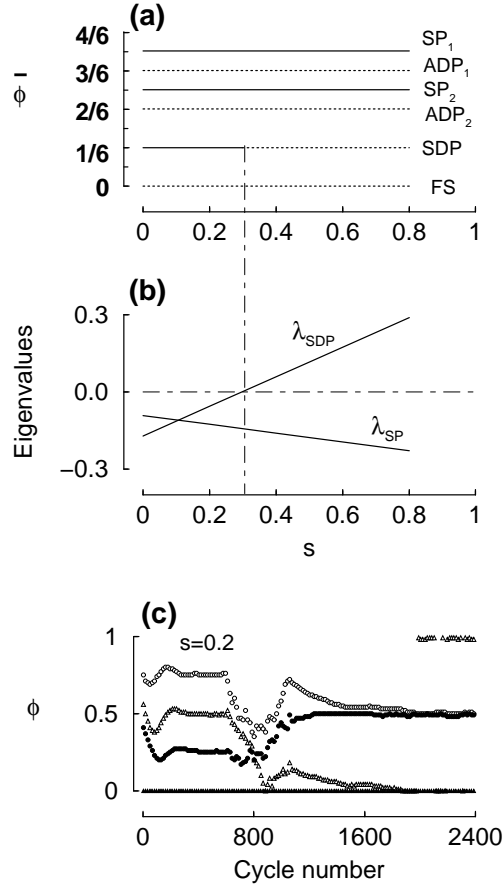


Figure 10: Co-existence and stability of six model-independent, phase-locked states in a network of four IF neurons with excitatory coupling (Fig. 1b). (a) The bifurcation diagram. The average phase difference for each state, defined by $\bar{\phi} = \frac{1}{3}(\phi_{21} + \phi_{31} + \phi_{42})$, is plotted as a function of s ($= w_I/w_O$). Solid lines are used for stable states and dotted lines for unstable ones. These states include one fully synchronous state (FS), one state of synchronous diagonal pairs (SDP), two states of anti-phase diagonal pairs (ADP₁, ADP₂), and two splay-phase states (SP₁, SP₂). (b) The s -dependent eigenvalues for the SDP and the SP states. The vertical, dash-dotted line indicates the value of s at which the SDP state becomes unstable. (c) Numerical result showing the transition from the SP state to the SDP state by increasing the noise intensity by 50 times for a finite period of time. This occurs when both SP and SDP are stable for $s = 0.2$. The parameter values used are given in Fig. 5.